Inorg. Chem. **2005**, *44*, 6019–6033

Solid-State Structures and Magnetic Properties of Halide-Bridged, Face-to-Face Bis-Nickel(II)-Macrocyclic Ligand Complexes: Ligand-Mediated Interchanges of Electronic Configuration

Konrad T. Szacilowski,[†,§] Puhui Xie,[†] Aramice Y. S. Malkhasian,[†] Mary Jane Heeg,[†] Manawadevi Y. Udugala-Ganehenege,[†] Lowell E. Wenger,[‡,||] and John F. Endicott*[,†]

Department of Chemistry, Wayne State University, Detroit, Michigan 48202-3929, and Department of Physics, University of Alabama at Birmingham, Birmingham, Alabama 35294-1170

Received January 28, 2005

Dramatic differences are found between the ambient and 100 K X-ray structures of $[L^{(2)}Ni_2Br_2](ClO_4)_2$ ($L^{(2)} = \alpha,\alpha'$-bis-{(5,7-dimethyl-1,4,8,11-tetraazacyclotetradeca-6-yl)-*o*-xylene), in which the bromide-bridged, bimetallic, macrocyclic ligand complexes of nickel(II) are held face-to-face and in which each bimetallic complex has a net triplet spin multiplicity. The ambient structure of this complex consists of very highly ordered, infinite chains of alternating *R* and *S* isomers in which the identical Ni(II) coordination spheres are near to the average expected for the high- and low-spin Ni(II) coordination sites, and there is appreciable stereochemical strain in the linkage of the macrocyclic ligands to the phenyl ring. In contrast, every other dinickel complex of the 100 K structure is displaced about 40 pm along the infinite chains to form tetrameric repeat units (pairs of dinickel complexes), in which each dinickel complex has well-defined high-spin and low-spin Ni(II) coordination sites; the high-spin sites are adjacent in the tetramers, and the stereochemical strain in the linkage to the phenyl spacer is relaxed. The molecular magnetic moments and structural contrasts are similar for the 100 K structure and the previously reported ambient structure of $[L^{(2)}Ni_2Br_3](ClO_4)$ complex for which the molecular magnetic moments also correspond to a single triplet state per complex. The halide-bridged, monochloro- and monobromo dinickel complexes also have triplet spin multiplicity, and they crystallize with a coordinated perchlorate completing the axial coordination of the high-spin Ni(II) site, while the other Ni(II) site of these halide-bridged complexes has equatorial Ni–N bond lengths typical of low-spin Ni(II) coordination. The bridging halide is sandwiched between the face-to-face macrocyclic ligand Ni(II) moieties and slightly off the Ni–Ni axis in all of the complexes. The temperature dependence of the magnetic moments of the series of complexes indicates that their singlet–triplet energy gaps are small, with zero point energy differences that are generally less than 10^3 cm^{-1}. The very weak metal–metal electronic coupling, the triplet state spin multiplicity of each dinickel complex, and the averaged high-spin/low-spin coordination environments of the ambient structure implicate a vibronic mechanism for the electronic configurational exchange in the dibromo and tribromo complexes. The single molecular vibrational mode that correlates with the configurational exchange in these complexes includes the concerted motion of the bridging bromide between the Ni(II) centers. Activation of this vibrational mode is sufficient to effect the configurational exchange. These complexes present especially clear examples of the effects of the coupling of nuclear vibrational motions to the interchange of electronic configuration between two different centers.

Introduction

The dynamic behavior of donor−acceptor (D/A) systems is well-known to be a function of the structural differences between the reactants and products and of the mixing between the reactant and product electronic configurations.[1−18] Thus, the rate constants for the transfer of electronic excitation energy and for the transfer of electronic charge

* To whom correspondence should be addressed. E-mail: jfe@chem.wayne.edu.
† Wayne State University.-
‡ University of Alabama at Birmingham.
§ Present address: Jagiellonian University, Faculty of Chemistry, Ingardena 3, 30-060 Kraków, Poland. E-mail: szacilow@chemia.uj.edu.pl.
|| E-mail: wenger@uab.edu.

(1) Marcus, R. A. *Discuss. Faraday Soc.* **1960**, *29*, 21.
(2) Marcus, R. A. *Annu. Rev. Phys. Chem.* **1964**, *15*, 155.
(3) Marcus, R. A. *J. Chem. Phys.* **1965**, *43*, 670.
(4) Hush, N. S. *Prog. Inorg. Chem.* **1968**, *8*, 391.
(5) Englman, R.; Jortner, J. *Mol. Phys.* **1970**, *18*, 145.
(6) Kuznetsov, A. M.; Ulstrup, J. Wiley-VCH: New York, 1998.

10.1021/ic050147x CCC: $30.25
Published on Web 07/21/2005

are both similarly dependent on the correlated nuclear displacements and the D/A electronic coupling.[13,19] The excitation energy transfer processes are often described as a combination of hole and electron-transfer processes.[13,20] In the simplest electron-transfer processes, the transfer of charge between the donor and acceptor centers is correlated with displacements in the positions of the nuclei near those centers and/or in the surrounding medium, and in the limit of weak electronic coupling, the charge-transfer event is treated as independent of the accompanying nuclear reorganization.[1−14] In contrast, experimental observations indicate that the nuclear and electronic motions are not independent in some systems in which the electronic coupling is strong,[14,21−23] and some related vibronic models for electron transfer have been proposed for D/A systems in which the electronic and nuclear motions are not separable.[24−26] This vibronic coupling limit is likely to be most important when the change of electronic configuration is accompanied by changes in the bond lengths to a bridging ligand.[14,23,27] The corresponding vibronic coupling limit has not been examined for excitation energy-transfer processes. The work reported here examines the influence of a halide-bridging ligand on the interchange of singlet and triplet electronic configurations between the nickel(II) centers of a bimetallic complex with a view to establish a relatively well-defined example of the vibronic coupling limit.

The synthesis and properties of tetraazamacrocyclic ligand complexes of Ni^{II} were thoroughly and well documented some time ago.[28−32] Complexes in which nickel(II) is coordinated by a 14-membered tetraaza-macrocyclic ligand

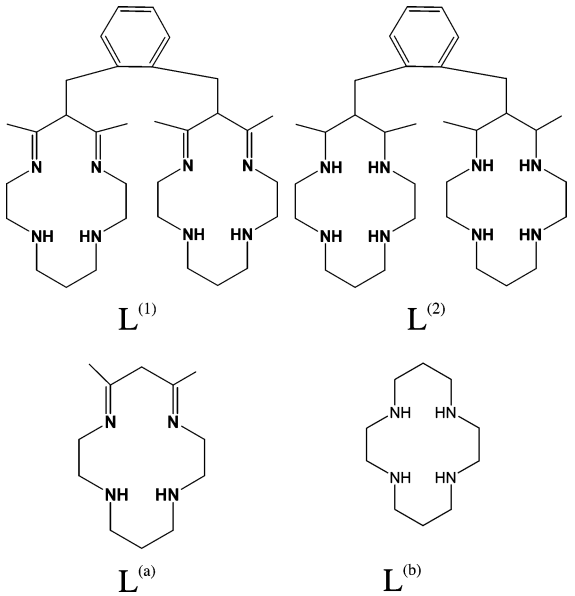

Figure 1. Skeletal structures of the ligands used in this study.

are reported to be either (1) four coordinate, approximately planar, and diamagnetic[28,29] or (2) six-coordinate tetragonal and paramagnetic in the presence of some halides and pseudo-halides.[28−30] The singlet−triplet energy difference is small in these complexes, and the higher energy electronic configuration can be populated by irradiation of the ligand field absorption bands to generate metastable intermediates that differ in coordination number and/or geometry from the ground state.[33] This geometrical difference results in a substantial nuclear reorganizational barrier to the change in electronic configuration, and one expects the recovery of the equilibrium distribution of species to be relatively slow, as in

$$[^1\mathrm{Ni}([14]\mathrm{aneN_4})]^{2+} + h\nu \rightarrow *[^3\mathrm{Ni}([14]\mathrm{aneN_4})]^{2+} \quad (1)$$

$$*[^3\mathrm{Ni}([14]\mathrm{aneN_4})]^{2+} + 2X^- \rightarrow [^3\mathrm{Ni}([14]\mathrm{aneN_4})X_2] \quad (2)$$

$$[^3\mathrm{Ni}([14]\mathrm{aneN_4})X_2] \rightarrow [^1\mathrm{Ni}([14]\mathrm{aneN_4})]^{2+} + 2X^- \quad (3)$$

where [14]aneN$_4$ = cyclam = 1,4,8,11-tetraazacyclotetradecane ($L^{(b)-}$ in Figure 1) and $h\nu = E_{ST}$ in Figure 2. The rates for the processes described by eq 2 amount to the relaxation of a vibrational excited state of $^3Ni^{II}$, and this should be very fast while the $[^3Ni([14]aneN_4)X_2]^{2+}$ relaxation process in eq 3 involves a change of geometry coupled to a change of electronic configuration. This process can be described in terms of a potential energy (PE) surface for each of the electronic configurations and a nuclear reorganizational

(7) Kestner, N.; Logan, J.; Jortner, J. *J. Phys. Chem.* **1974**, *64*, 2148.
(8) Cannon, R. D. *Electron Transfer Reactions*; Butterworth: London, 1980.
(9) Richardson, D. E. In *Inorganic Electronic Structure and Spectroscopy*; Solomon, E. I., Lever, A. B. P., Eds.; Wiley: New York, 1999; Vol. II, p 131.
(10) Meyer, T. J.; Taube, H. In *Comprehensive Coordination Chemistry*; Wilkinson, G., Ed.; Pergamon: Oxford, U.K., 1987; Vol. 7, p 331.
(11) Newton, M. D.; Sutin, N. *Annu. Rev. Phys. Chem.* **1984**, *35*, 437.
(12) Piotrowiak, P. *Chem. Soc. Rev.* **1999**, *28*, 143.
(13) Piotrowiak, P. In *Electron Transfer in Chemistry*; Balzani, V., Ed.; Wiley-VCH: Weinheim, Germany, 2001; Vol. 1, p 215.
(14) Endicott, J. F. In *Comprehensive Coordination Chemistry II, Vol. 7*, 2nd ed.; McCleverty, J., Meyer, T. J., Eds.; Pergamon: Oxford, U.K., 2003; Vol. 7, p 657.
(15) Newton, M. D. *Chem. Rev.* **1991**, *91*, 767.
(16) Newton, M. D. *Adv. Chem. Phys.* **1999**, *106*, 303.
(17) Newton, M. D. In *Electron Transfer In Chemistry*; Balzani, V., Ed.; Wiley-VCH: Weinheim, Germany, 2001; Vol. 1, p 3.
(18) Sumi, H. In *Electron Transfer in Chemistry, Vol. 1*; Balzani, V., Ed.; Wiley-VCH: Weinheim, Germany, 2001; Vol. 1, p 65.
(19) Endicott, J. F.; Ramasami, T.; Gaswick, D. C.; Tamilarasan, R.; Heeg, M. J.; Brubaker, G. R.; Pyke, S. C. *J. Am. Chem. Soc.* **1983**, *105*, 5301.
(20) Turro, N. *Modern Molecular Photochemistry*; Benjamin/Cummings: Menlo Park, CA, 1978.
(21) Watzky, M. A.; Macatangay, A. V.; Van Camp, R. A.; Mazzetto, S. E.; Song, X.; Endicott, J. F.; Buranda, T. *J. Phys. Chem.* **1997**, *101*, 8441.
(22) Macatangay, A. V.; Endicott, J. F. *Inorg. Chem.* **2000**, *39*, 437.
(23) Brunold, T. C.; Gamelin, D. R.; Solomon, E. L. *J. Am. Chem. Soc.* **2000**, *122*, 8511.
(24) Piepho, S. B.; Krausz, E. R.; Schatz, P. N. *J. Am. Chem. Soc.* **1978**, *100*, 2996.
(25) Piepho, S. B. *J. Am. Chem. Soc.* **1990**, *112*, 4197.
(26) Schatz, P. N. In *Inorganic Electronic Structure and Spectroscopy*; Solomon, E. I., Lever, A. B. P., Eds.; Wiley: New York, 1999; Vol. II, p 175.
(27) Schwarz, C. L.; Endicott, J. F. *Inorg. Chem.* **1995**, *34*, 4572.
(28) *Coordination Chemistry of Macrocyclic Compounds*; Melson, G. A., Ed.; Plenum: New York, 1979.
(29) Martin, L. Y.; Sperati, C. R.; Busch, D. H. *J. Am. Chem. Soc.* **1977**, *99*, 2968.
(30) Prasad, L.; Nyberg, S. C.; McAuley, A. *Acta Crystallogr.* **1987**, *C43*, 1038.
(31) Bosnich, B.; Mason, R.; Pauling, P. J.; B., R. G.; Tobe, M. L. *J. Chem. Soc., Chem. Commun.* **1965**, 97.
(32) Prasad, L.; McAuley, A. *Acta Crystallogr.* **1983**, *C39*, 1175.
(33) Campbell, L.; McGarvey, J. J.; Samman, N. G. *Inorg. Chem.* **1978**, *17*, 3378.

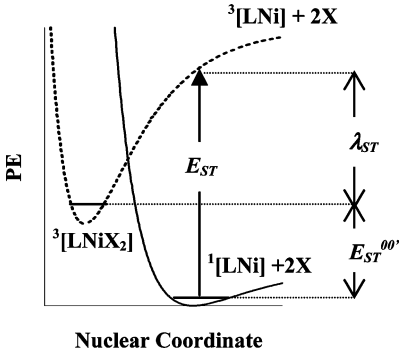

Figure 2. Qualitative PE diagram illustrating the energy parameters for a low-spin Ni^{II} complex associating with weakly bonding ligands.

barrier to their interconversion so that the $[^3Ni([14]aneN_4)X_2]^{2+}$ intermediate should have a relatively long lifetime even though it is not the thermodynamically stable form of the Ni^{II} complex; see Figure 2. In view of these considerations, it is interesting that Kajiwara et al., recently found only one high-spin Ni(II) center in a dinickel tribromide complex, $[L^{(2)}Ni_2Br_3]^+$, in which each Ni(II) center is nominally six-coordinate in the solid state (with two axial bromides outside the bimetallic complex, a bridging bromide, and each Ni^{II} coordinated equatorially by a tetraazamacrocyclic ligand).[34] These authors' further observations that the Ni^{II} centers of the bromide- and chloride-bridged[35] dinickel complexes had bond distances that appeared to be the average of those expected for the high- and low-spin configurations of Ni(II) and of only weak magnetic coupling between the metal centers suggest that either (1) the singlet−triplet configurational interchange in these complexes is relatively rapid (very small nuclear reorganizational barrier) or (2) the complexes are electronically disordered in the crystal lattice.

The bridging-halide-mediated electronic coupling between dσ-donor and dσ-acceptor metal centers has long been presumed to be a very effective major factor in some very facile inner-sphere electron-transfer reaction pathways[8,10,14,27,36−39] and in the unusual properties of $(M^{II}-X-M^{IV}-X)_n$ and $(M^{III}-X-M^{III}-X)_n$ chains in the solid state (M = Pt or Pd in the former and Ni in the latter).[40−44] However, there have been few simple, halide-bridged complexes that permit a systematic evaluation of the coupling of transition-metal D/A complexes through σ-networks. This is in marked contrast to the many simple models for D/A coupling through π-networks.[9,10,45−51] While one might expect some differences between hole- and electron-transfer mechanisms for D/A coupling when comparing the σ- and π-bridged D/A systems,[50] it has been proposed[27] that halide-bridged electron-transfer systems may actually be examples of vibronically induced mixing of the D and A electronic configurations by means of the concerted motion of the bridging ligand between reactant centers.[9,24,25,52,53]

The electronic coupling in a σ-bridged D/A system can be treated in terms of a three-center, perturbation-theory model.[54] This approach treats the electronic coupling in terms of the overlap of the donor orbital and the acceptor orbital with some bridging-ligand orbital, and it leads to antiferromagnetic coupling in the network of coupled orbitals. Related arguments have been used to rationalize reactivity patterns in thermal kinetic studies in which the metal complexes are equatorially coordinated by tetraaza-macrocyclic ligands.[27,39] However, very little magnetic coupling has been found in the face-to-face, xylene linked bimetallic complexes, $[L^{(k)}M_2X_n]^{(4-n)+}$ (X = Cl or Br for M = Cu^{II} and $k = 1$ or for M = Ni^{II} and $k = 2$; see Figure 1).[34,35,54−56] Furthermore, the description of the relevant three-center interaction is most readily formulated in terms of the halide-mediated configurational mixing of the ground state with a $\{Ni^{I},Ni^{III}\}$ metal-to-metal charge-transfer (MMCT) excited state.[54] This model predicts that the strength of the interaction should increase as the ionization energy of the bridging halide decreases. However, the $[L^{(2)}Ni_2X_n]^{(4-n)+}$ complexes do not have intense, low-energy MMCT absorption bands suggesting that metal−metal electronic coupling in these halide-bridged complexes is weak.[56] Our observations indicate that most, but not all, of the $[LNi_2X_4]$ complexes are paramagnetic in solution[56] and qualitatively in accordance with the earlier observations on the analogous dihalide solids.[28,29,57] These and other observations confirm that the Ni^{II} singlet and triplet electronic configurations ($e^4a_1^2b_2^2$, and $e^4b_2^2a_1b_1$, or possibly $e^4a_1^2b_2b_1$, respectively, in axial C_{4v} symmetry) do not differ much in energy. In this report, we have examined the solid-

(34) Kajiwara, T.; Yamaguchi, T.; Kido, H.; Kawabuta, S.; Kuroda, R.; Ito, T. *Inorg. Chem.* **1993**, *32*, 4990.
(35) Kajiwara, T.; Yamaguchi, T.; Oshio, H.; Ito, T. *Bull. Chem. Soc. Jpn.* **1994**, *67*, 2130.
(36) Taube, H.; Myers, H.; Rich, R. L. *J. Am. Chem. Soc.* **1953**, *75*, 4118.
(37) Taube, H. In *Mechanistic Aspects of Inorganic Reactions*; Rorabacher, D. B., Endicott, J. F., Eds.; ACS Symposium Series 198; American Chemical Society: Washington, DC, 1982; p 151.
(38) Taube, H. *Can. J. Chem.* **1959**, *37*, 129.
(39) Rotzinger, F. P.; Kumar, K.; Endicott, J. F. *Inorg. Chem.* **1982**, *21*, 4111.
(40) Clark, R. J. H. *Chem. Soc. Rev.* **1984**, *13*, 219.
(41) Clark, R. J. H. In *Vibronic Processes in Inorganic Chemistry*; Flint, C. D., Ed.; Kluwer Academic Publishers: Dordrecht, Germany, 1989; p 301.
(42) Toriumi, K.; Wada, Y.; Mitami, T.; Bandow, S.; Yamashita, M.; Y., F. *J. Am. Chem. Soc.* **1989**, *111*, 2341.
(43) Yamashita, M.; Manabe, T.; Inoue, K.; Kawashima, T.; Okamoto, H.; Kitigawa, H.; Mitami, T.; Toriumi, K.; Miyamae, H.; Ikeda, R. *Inorg. Chem.* **1999**, *38*, 1894.
(44) Manabe, T.; Yokoyama, K.; Sachie, F.; Kachi-Terajima, C.; Nakata, K. F. I.; Miyasaka, H.; Suguira, K.; Yamashita, M.; Kishida, H.; Okamoto, H. *Inorg. Chem.* **2002**, *41*, 4993.
(45) Creutz, C. *Prog. Inorg. Chem.* **1983**, *30*, 1.
(46) Crutchley, R. *Adv. Inorg. Chem.* **1994**, *41*, 273.
(47) Richardson, D. E.; Sen, J. P.; Taube, H. *Inorg. Chem.* **1982**, *21*, 3136.
(48) Richardson, D. E.; Taube, H. *J. Am. Chem. Soc.* **1983**, *105*, 40.
(49) Richardson, D. E.; Taube, H. *Coord. Chem. Rev.* **1984**, *60*, 107.
(50) Creutz, C.; Newton, M. D.; Sutin, N. *Photochem. Photobiol., A* **1994**, *82*, 47.
(51) Creutz, C.; Brunschwig, B. S.; Sutin, N. In *Comprehensive Coordination Chemistry II*; McCleverty, J., Meyer, T. J., Eds.; Elsevier: Amsterdam, The Netherlands, 2004; Vol. 7, p 731.
(52) Schatz, P. N. In *Inorganic Electronic Structure and Spectroscopy Vol. II*; Solomon, E. I., Lever, A. B. P., Eds.; Wiley: New York, 1999; p 175.
(53) Stritar, J.; Taube, H. *Inorg. Chem.* **1969**, *8*, 2281.
(54) Ugudala-Ganehenege, M. Y.; Heeg, M. J.; Hryhorczuk, L. M.; Wegner, L. E.; Endicott, J. E. *Inorg. Chem.* **2001**, *40*, 1614.
(55) Ugudala-Ganehenege, M. Y. Ph.D. Dissertation, Wayne State University, Detroit, MI, 2000.
(56) Szacilowski, K.; Udugala-Ganenenege, M. Y.; Endicott, J. F. Unpublished work.
(57) Urbach, F. L. In *Coordination of Macrocyclic Compounds*; Melson, G. A., Ed.; Plenum: New York, 1979; p 345.

Table 1. Elemental Analysis of the Dinickel Complexes

complexes	molecular formula	% weight (theory)	% weight (found)
$[(L^{(2)}Ni_2)(ClO_4)](ClO_4)_3$	$C_{32}H_{62}Cl_4N_8Ni_2O_{16}$	C, 35.78; H, 5.82; N, 10.43	C, 35.18; H, 5.75; N, 10.02
$[(L^{(2)}Ni_2)Cl(ClO_4)](ClO_4)_2$	$C_{32}H_{62}Cl_4N_8Ni_2O_{12}$	C, 38.05; H, 6.19; N, 11.09	C, 38.83; H, 6.41; N, 10.99
$[(L^{(2)}Ni_2)Br(ClO_4)](ClO_4)_2$	$C_{32}H_{62}Cl_3BrN_8Ni_2O_{12}$	C, 36.41; H, 5.88; N, 10.62	C, 36.79; H, 5.98; N, 10.51
$[(L^{(2)}Ni_2)I](ClO_4)_3$	$C_{32}H_{62}ICl_3N_8Ni_2O_{12}$	C, 34.89; H, 5.67; N, 10.17	C, 35.06; H, 5.70; N, 9.91
$\{[(L^{(2)}Ni_2)Br_2](ClO_4)H_2O\}_n$	$C_{32}H_{64}Cl_2Br_2N_8Ni_2O_9$	C, 36.47; H, 6.08; N, 10.63	C, 37.12; H, 5.97; N, 10.78
$[(L^{(2)}Ni_2)Br_3]ClO_4$	$C_{32}H_{62}Br_3ClN_8Ni_2O_4$	C, 37.85; H, 6.15; N, 11.03; Br, 23.61	C, 38.20; H, 6.10; N, 10.94;Br, 22.76

state properties of some of the halide-bridged dinickel complexes in order to gain some insight into the behavior of these systems.

Experimental Section

Materials. Nickel acetate tetrahydrate, α,α′-dibromoxylene, acetylacetone, and *N*,*N*′-bis(etylenediamine)propylenediamine were supplied by Aldrich and used as received. The (5,7-dimethyl-1,4,8,-11-tetraazacyclotetradeca-4,7-dieno(−1))nickel(II) complex, $[L^{(a)}Ni]NO_3$, was prepared according to a previously described procedure[58] (ligand structures in Figure 1).

α,α′-Bis{(5,7-dimethyl-1,4,8,11-tetraazacyclotetradeca-4,7-diene-6-yl)nickel}-*o*-xylene ($[L^{(1)}Ni_2]^{4+}$) Perchlorate. A 7.125 g quantity of $[L^{(a)}Ni]NO_3$ was combined with 2.7 g of dibromoxylene and dissolved in 375 mL of anhydrous ethanol. This solution was refluxed for 6 h and filtered. The volume of the filtrate was reduced to 225 mL, added slowly to 75 mL of acidified (1.5 mL of concentrated perchloric acid) saturated aqueous $NaClO_4$, stirred vigorously, and cooled with ice water for 2 h. The crude product was recrystallized from hot water acidified with perchloric acid (approximately a 47:3 volume ratio of $H_2O/HClO_4$).

Caution: The use of perchlorates in these preparations is potentially hazardous.

α,α′-Bis{(5,7-dimethyl-1,4,8,11-tetraazacyclotetradeca-6-yl)-nickel}-*o*-xylene ($[L^{(2)}Ni_2]^{4+}$) Perchlorate. A 2.7 g sample of $[L^{(1)}Ni_2](ClO_4)_4$ (∼10 mmol) was dissolved in 150 mL of hot 50% ethanol acidified with 3 mL of concentrated $HClO_4$, then 4.5 g of solid $NaBH_4$ was added slowly while stirring vigorously. The solution pH was kept ≤5 by the additions of $HClO_4$ (maximum ∼33 mL). An orange-red suspension formed, and the mixture was refluxed for 5−10 min, then cooled, and the orange product was separated. The product was purified by recrystallization. ESI: 971.23, $[M - ClO_4]^{3+}$; 871.27, $[M - ClO_4 - HClO_4]^{2+}$; 771.31 $[M - ClO_4 - 2HClO_4]^{+}$. IR (3207 cm^{-1}, ν_{N-H}).

Halide-Bridged (−Cl, −Br, −I) Complexes Derived from $[L^{(2)}Ni_2]^{4+}$. About 150 mg of $[L^{(2)}Ni_2](ClO_4)_4$ was dissolved in about 10 mL of hot 50% aqueous ethanol. Molar equivalent amounts of NH_4Cl, NH_4Br, or NH_4I were dissolved in a small amount of 50% aqueous ethanol, then the solution was mixed quickly with the hot solution of $[L^{(2)}Ni_2](ClO_4)_4$. The bottles were sealed and immersed in a small Dewar flask filled with boiling water. Crystals formed after 1−3 days. The crystals were forced out by adding 96% ethanol. Molar ratios of 1:2 and 1:3 $[L^{(2)}Ni_2](ClO_4)_4$ to NH_4Br were used to prepare the di-Br- and tri-Br-bridged dinickel complexes, respectively.

The elemental analyses, summarized in Table 1, were performed by Midwest Microlab, LLC (Indianapolis, IN).

Magnetic Measurements. Magnetic susceptibility measurements were made on pulverized samples using a Quantum Design model MPMS-5S SQUID magnetometer over a temperature range of 5−350 K with a field strength of 5000 Oe. The molar susceptibilities calculated for the dinickel complexes were corrected for the core diamagnetism (approximately -570×10^{-6} emu mol^{-1}) and a temperature-independent paramagnetic contribution (150×10^{-6} emu mol^{-1}). The reliability of these corrections was independently verified as the corrections were within 5% of the measured susceptibility for the $[L^{(2)}Ni_2]^{4+}$ perchlorate sample, a sample that had no magnetic contribution from the Ni(II) ions (both Ni(II) centers were in the $S = 0$ state).

Both the zero-field-cooled magnetization (ZFCM) and the field-cooled magnetization (FCM) were determined. The ZFCM is measured after cooling the sample from room temperature to 5 K in the absence of a magnetic field, applying the 5000 Oe field, and then warming (discrete temperature steps and waiting for the temperature to stabilize). FCM is measured during warming after cooling the sample down to 5 K in the presence of the 5000 Oe field.

X-ray Structure Determinations. Diffraction data were collected on a Bruker P4/CCD or APEX II diffractometer equipped with Mo Kα radiation and a graphite monochromator. The manufacturer's[59] software was used for processing. A complete sphere of data was collected at 10 s/frame and 0.2 or 0.3° between frames. The structures were solved and refined with Sheldrick's SHELX-97.[60] The SQUEEZE portion of Spek's PLATON[61,62] software was used to place disordered anions and solvent when noted. The crystallographic parameters are summarized in Table 2.

Results

The perchlorate salts of the complexes with unsaturated ligands are yellow, while the low-spin complexes $[L^{(b)}Ni]^{2+}$ and $[L^{(2)}Ni_2]^{2+}$ with saturated ligands (see Figure 1) are orange. The halide-bridged complexes are very easily formed by mixing solutions containing $[L^{(n)}Ni_2]^{2+}$ with halide salts, and the formation constants of the l:1 complexes of $[L^{(1)}Ni_2]^{2+}$ with chloride or bromides are large ($\geq 10^4$ m^{-1}). However, we were not able to isolate X-ray quality solids. The salts of the halide-bridged complexes are relatively dark and vary from red to purple. The X-ray crystal structures of these salts are more varied than one might expect for simple substitutions of halides. The low-temperature magnetic properties of the complexes in the solid state vary from paramagnetic with one high-spin Ni(II) center per bimetallic unit (for the Cl- and Br-bridged $[L^{(2)}Ni_2]^{2+}$ complexes) to diamagnetic for the perchlorate salts of the $[L^{(n)}Ni_2]^{2+}$ complexes and for the I-bridged $[L^{(2)}Ni_2]^{2+}$ complex. The Ni/Ni magnetic coupling seems to be negligible in all of the complexes that we examined.

(58) Martin, J. G.; Cummings, S. C. *Inorg. Chem.* **1973**, *12*, 1477.

(59) *SMART, S. a. S.* are collection programs distributed by the manufactures, Brucker AXS Inc., Madison, WI.

(60) Sheldrick, G. In *SHELX-97*; University of Gottingen: Gottingen, Germany, 1997.

(61) Spek, A. L. In *PLATON*; Utrecht University: The Netherlands, 2003.

(62) Spek, A. L. *J. Appl. Crystallogr.* **2003**, *36*, 7.

Table 2. Crystallographic Parameters

	$[L^{(2)}Ni_2Cl(ClO_4)](ClO_4)_2 \cdot H_2O$[a]	$\{L^{(2)}Ni_2I\](ClO_4)_3$[b]	$[L^{(2)}Ni_2Br(ClO_4)](ClO_4)_2 \cdot 0.5\ HOCH_2CH_3$[c]	$[L^{(2)}Ni_2Br_2](ClO_4)_2 \cdot H_2O$[d]	$[L^{(2)}Ni_2Br_2](ClO_4)_2 \cdot H_2O$[e]	$[L^{(2)}Ni_2Br_3]Br \cdot H_2O$	$[L^{(1)}Ni_2](ClO_4)_4 \cdot 1.5\ H_2O$[f]	$[L^{(2)}Ni_2(ClO_4)](ClO_4)_3 \cdot H_2O \cdot HOCH_2CH_3$[g]
empirical formula	$C_{32}H_{64}Cl_4N_8Ni_2O_{13}$	$C_{32}H_{62}Cl_3IN_8Ni_2O_{12}$	$C_{33}H_{65}BrCl_3N_8Ni_2O_{12.5}$	$C_{32}H_{64}Br_2Cl_2N_8Ni_2O_9$	$C_{32}H_{64}Br_2Cl_2N_8Ni_2O_9$	$C_{32}H_{64}Br_4N_8Ni_2O$	$C_{32}H_{57}Cl_4N_8Ni_2O_{17.5}$	$C_{34}H_{70}Cl_4N_8Ni_2O_{18}$
formula weight	1028.13	1101.57	1077.61	1053.02	999.07	1013.97	1093.08	1138.20
temperature	295(2) K	295(2) K	193(2) K	295(2)K	100(2) K	100(2) K	295(2) K	295(2) K
wavelength	0.71073 Å	0.71073 Å	0.71073 Å	0.71073 Å	0.71073 Å	0.71073 Å	0.71073 Å	0.71073 Å
crystal system, space group	monoclinic, $P2_1/n$	orthorhombic, *Pbcn*	monoclinic, $P2_1/n$	orthorhombic, *Ima*2 (no. 46)	orthorhombic, *Cmc*21	monoclinic, $P2_1/c$	monoclinic, $P2_1/c$	monoclinic, $P2_1/c$
unit cell dimensions	$a = 11.2071(2)$ Å, $b = 23.884(5)$ Å, $c = 17.648(3)$ Å, $\beta = 100.896(5)°$	$a = 25.311(2)$ Å, $b = 18.5001(13)$ Å, $c = 20.4973(17)$ Å	$a = 11.253(2)$ Å, $b = 23.910(5)$ Å, $c = 17.381(4)$ Å, $\beta = 102.474(7)°$	$a = 23.084(3)$ Å, $b = 9.3783(11)$ Å, $c = 20.097(3)$ Å	$a = 23.3664(6)$ Å $b = 18.7097(6)$ Å $c = 20.0991(6)$ Å	$a = 9.1751(5)$ Å, $b = 20.702\ 1(13)$ Å, $c = 20.7219(13)$ Å, $\beta = 95.941(3)°$	$a = 20.384(3)$ Å, $b = 13.368(2)$ Å, $c = 33.608(6)$ Å, $\beta = 91.505(3)°$	$a = 18.781(4)$ Å, $b = 9.3430(18)$ Å, $c = 28.009(6)$ Å, $\beta = 97.421(2)°$
volume	4638.7(15) Å^3	9598.0(13) Å^3	4566.2(16) Å^3	4350.8(10) Å^3	8786.9(4) Å^3	3914.9(4) Å^3	9155(3) Å^3	4873.7(17) Å^3
Z, calculated density	4, 1.472 g cm^{-3}	8, 1.525 g cm^{-3}	4, 1.568 g cm^{-3}	4, 1.580 g cm^{-3}	8, 1.619 g cm^{-3}	4, 1.720 g cm^{-3}	8, 1.586 g cm^{-3}	4, 1.551 g cm^{-3}
absorption coefficient	1.107 mm^{-1}	1.655 mm^{-1}	1.941 mm^{-1}	2.988 mm^{-1}	semiempirical from equivalents	5.082 mm^{-1}	1.134 mm^{-1}	1.069 mm^{-1}
crystal size	$0.25 \times 0.16 \times 0.10$ mm^3	$0.30 \times 0.18 \times 0.10$ mm^3	$0.20 \times 0.10 \times 0.10$ mm^3	$0.40 \times 0.20 \times 0.10$ mm^3	$0.30 \times 0.25 \times 0.12$ mm^3	$0.16 \times 0.12 \times 0.05$ mm^3	$0.60 \times 0.40 \times 0.15$ mm^3	$0.30 \times 0.06 \times 0.06$ mm^3
Final R indices [$I > 2\sigma(I)$]	$R_1 = 0.080$, $wR_2 = 0.199$	$R_1 = 0.035$, $wR_2 = 0.078$	$R_1 = 0.092$, $wR_2 = 0.240$	$R_1 = 0.050$, $wR_2 = 0.127$	$R_1 = 0.0339$, $wR_2 = 0.0911$	$R_1 = 0.0521$, $wR_2 = 0.1295$	$R_1 = 0.080$, $wR_2 = 0.247$	$R_1 = 0.091$, $wR_2 = 0.199$
R indices (all data)	$R_1 = 0.181$, $wR_2 = 0.222$	$R_1 = 0.091$, $wR_2 = 0.085$	$R_1 = 0.177$, $wR_2 = 0.268$	$R_1 = 0.075$, $wR_2 = 0.135$	$R_1 = 0.0448$, $wR_2 = 0.932$	$R_1 = 0.0790$, $wR_2 = 0.1409$	$R_1 = 0.1548$, $wR_2 = 0.283$	$R_1 = 0.321$, $wR_2 = 0.272$

[a] There is an ill-defined region that contained two perchlorate anions and one water molecule that were occupied by electrons calculated by SQUEEZE, so that two independent perchlorates and one water will not be listed in the atomic tables. [b] A difference map showed all three of the perchlorate anions, but refinement resulted in unreasonable chemical geometry. Therefore, this electronic region was calculated by SQUEEZE. [c] Two sets of partial atoms were held isotropic to describe one ethylenediamine linkage (C6 and C7). The anions and solvent were disordered. Two out of the three perchlorate anions, and the half ethanol, were included as SQUEEZE'd contributions. [d] Two-half perchlorates were added to the asymmetric unit by SQUEEZE; one was on the mirror and another on the two-fold axis, but both were badly disordered. The model refined with 19% racemic twinning. The Br anions create a bridging polymeric structure. The bridging phenyl ring occupies a crystallographic mirror, one bridging Br atom is on another mirror and one bridging Br atom is on the two-fold axis. [e] One and one-half perchlorates and two water molecules were added to the asymmetric unit by SQUEEZE. Both the perchlorates and water were badly disordered. [f] The anions and solvent were disordered. No hydrogen atoms were placed on the water solvent. [g] The anions and solvent were badly disordered. Partial atoms were held isotropic to describe some perchlorato oxygen atoms. No hydrogen atoms were placed on the water solvent. These needles were badly twinned and multiple data collections resulted in this best model. The identity of the compound is undoubtedly assigned correctly, but small variations in geometry may not be significant.

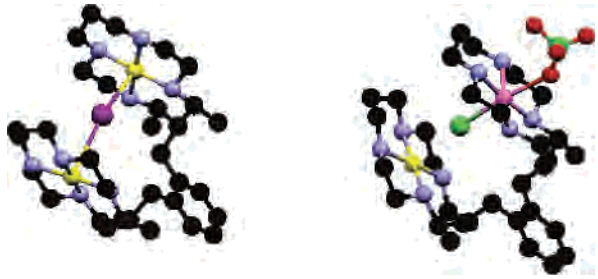

Figure 3. Structures of monohalo complexes: iodo, left; chloro, right.

X-ray Structures of the $[(L^{(2)}Ni_2)X](ClO_4)_3$ Complexes (X = Cl, Br, I). We have found two different types of molecular structure for these complexes as shown in Figure 3; all of the structures in this report have been drawn using Mercury l.2.1, and the hydrogen atoms have been omitted for clarity. The monoiodo complex is diamagnetic, and the iodide is equidistant from the Ni centers (Ni−I−Ni angle of 161°) in the $[(L^{(2)}Ni_2)I]^{3+}$ complex, and the perchlorates are well removed from the coordination spheres of the metals. This structure is analogous to the structures found for the $[(L^{(1)}Cu_2)X]^{3+}$ complexes (X = Cl or Br).[54] The Ni−N bond lengths for the monoiodo complex are very close to the 194 pm expected for equatorial bond lengths in low-spin Ni(II).

The monochloro and monobromo complexes have structures that are very similar to one another with one six-coordinate Ni^{II} center and one four- or five-coordinate (depending on how the bridging halide is classified) Ni^{II} center; as is expected for one high-spin and one low-spin Ni(II) center in each complex, the Ni−N bond lengths average 206 and 194 pm, respectively. The Ni−Ni distances within the $L^{(2)}$ moiety increase from Cl to I and are 10−20% more than the differences in ionic diameters.[63] The X-ray parameters are summarized in Tables 2 and 3.

295 K X-ray Structure of $\{[(L^{(2)}Ni_2)Br_2](ClO_4)_2\cdot H_2O\}_n$. The structure of this complex at 295 K is comprised of very well-ordered, infinite, one-dimensional chains (the $[-Ni-Br-Ni-Br-]_n$ axis, see Figure 4) in which the *R* and *S* optical isomers alternate. The xylene-linked, dinickel moieties within the infinite chain have coordination sphere bond distances that are very similar to those in the ambient molecular structure of $[(L^{(2)}Ni_2)Br_3]Br$ reported by Kajiwara et al.;[34] see Table 3. The bridging bromide within the dinickel complex moiety is disordered along the Ni−Br−Ni axis, but this bromide is required to be centered by the crystal symmetry and $d_{Ni-Br} = 291$ pm. Each Ni(II) center has the same coordination environment with averaged high-spin/low-spin coordination sphere bond distances; yet the magnetic measurements indicate that there is one singlet Ni(II) and one triplet Ni(II) per complex. The dihedral angles of the xylene linkage (apical carbon of the MCL ligand, linking methylene, adjacent C−C edge of the phenyl ring) are much smaller (∼15°) than those in the other complexes (∼50−60°), and the molecular symmetry of the dinickel moiety is nearly C_{2v}. This is the most ordered structure found for any complex in this series. The compression of the dihedral angles around the linking methylenes and possibly the averaged Ni^{II}-ligand bond lengths indicate that the structure is stereochemically strained.

100 K X-ray Structure of $\{[(L^{(2)}Ni_2)Br_2](ClO_4)_2\cdot H_2O\}_n$. After several unsuccessful attempts, we obtained a low-temperature X-ray structure of a $\{[(L^{(2)}Ni_2)Br_2](ClO_4)_2\}_n$ crystal. This structure is also comprised of infinite (−Ni−Br−Ni−Br−) chains, but it has very well-defined singlet and triplet Ni^{II} coordination sites with a shorter distance between the triplet Ni^{II} centers than the singlet centers of neighboring dinickel complexes. Figure 5 compares the 295 and 100 K molecular structures along the infinite chains. The unit cell of the 100 K structure has slightly more than twice the volume of the 295 K structure. The structure of $\{[(L^{(2)}Ni_2)Br_2](ClO_4)_2\}_n$ at 100 K differs from that at 295 K in (1) the 30 pm difference in external Ni−Br bond lengths, (2) the relaxation of the stereochemical strain around the xyleyne linkage (53° dihedral angles of the linking methylenes), (3) the 10 pm difference in Ni−N bond lengths found for the two Ni centers (in the 100 K structure in contrast to the nearly identical bond lengths of the 295 K structure), and (4) the average 18 pm difference in positions of the Ni-macrocyclic ligand moieties along the infinite chains. In view of these differences in the structures, it is remarkable that the Ni−Ni distances within their dinickel moieties are identical. The structural differences are large enough that they amount to a phase change. Overall, the 100 K structure is very similar to the structure reported for $[(L^{(2)}Ni_2)Cl_2](ClO_4)_2$.[35]

100 K X-ray Structure of $[(L^{(2)}Ni_2)Br_3]ClO_4$. This structure shows one high-spin Ni(II) with long Ni−N (207 pm) and short Ni−Br bonds (262 and 271 pm inside and outside the dimer, respectively), and one low-spin Ni(II) with short Ni−N (196 pm) and long Ni−Br (332 and 307 pm) bonds. The dinickel complexes in this structure are arrayed with the *R* and *S* isomers alternating along the crystallographic *c*-axis and the singlet and triplet Ni^{II} centers of the dinickel complexes alternating along the *b*-axis; see Figure 6. This structure differs from the 300 K structure of Kajiwara et al.,[34] in that *both* axial, Ni−Br, bond lengths are shorter and the equatorial, Ni−N, bond lengths are significantly longer at one Ni center than at the other.

X-ray Structures of the $[L^{(n)}Ni_2](ClO_4)_4$ Salts ($n = 1, 2$). These structures illustrate the flexibility of the linkage between the MCL moieties of the complexes. In the $[L^{(1)}Ni_2](ClO_4)_4$ complex, the MCL-complex moieties are rotated to positions above and below the xylene linker, Figure 7. In the $[(L^{(2)}Ni_2)ClO_4](ClO_4)_3$ structure, the MCL-complex moieties are far enough apart to accommodate an intercalated perchlorate. This suggests that the diimine−diamine macrocyclic ligand moieties are more rigid, and/or there is a competing contribution from $\pi-\pi$ stacking that makes the intercalation of the perchlorate anion less favorable than that in the tetraamine analogue. The Ni−N(amine) distances in the equatorial macrocyclic ring average 194 pm in both complexes, as is characteristic of low-spin Ni^{II} in macrocyclic

(63) Huheey, J., *Inorganic Chemistry*, 2nd ed.; Harper and Row: New York, 1978.

Table 3. Summary of Ni Coordination Sphere Structural Data from the X-ray Crystal Structures of Xylene-Linked Bis-Macrocyclic Ligand Complexes

	M−N bond lengths:			M−X bond lengths:			
complex[b]	low spin $d_{M(l)-N}$,[a] pm	intermediate d_{M-N},[a] pm	high spin $d_{M(h)-N}$,[a] pm	low spin $d_{M(l)-X}$,[c] pm	intermediate $d_{M(h)-X}$,[c] pm	high spin $d_{M-M'}$,[d] pm	Ni−X−Ni, deg
$[(L^{(2)}Ni_2)(ClO_4)Cl]^{2+}$	194(2)		206.1(0.5)	334 (Cl)	244 (Cl) 238 (O)	571 (in) 920 (out)	169.6
$\{[(L^{(2)}Ni_2)(Cl)_2]\}_2^{2+}$[e]		199(1)	204(2)	286 (in)[f] 328 (out)[g]	257 (in)[f] 258 (out)[h]	542 (in) 532 (out)[i] 585 (out)[j]	
$[(L^{(2)}Ni_2)(ClO_4)Br]^{2+}$[k] (193 K)	194(2)		207(4)	328 (Br)	259 (Br) 231 (O)[l]	584 (in) 920 (out)	169.2
$\{[(L^{(2)}Ni_2)(Br)_2]^{2+}\}_n$		202(2)			291 (in)[m] 287 (out)	581 (in) 575 (out)	173.2
$\{[(L^{(2)}Ni_2)(Br)_2]^{2+}\}_n$ (100 K)	195.5 (0.5)		207 (1)	326 (in) 319 (out)	261 (in) 273 (out)	586 (in) 545 (out)[i] 622 (out)[j]	170.6
$[(L^{(2)}Ni_2)(Br)_3]^{+}$[n]		201(1)		326 (in)[f] 288 (out)	257 (in)[f] 288 (out)	580 (in) 740 (out)	167.4
$[(L^{(2)}Ni_2)(Br)_3]^{+}$ (100 K)	195.6 (1.2)		206.8 (0.5)	332.2 (in) 306.7 (out)	262.3 (in) 270.6 (out)	580 (in) 737 (out)	154.6
$[(L^{(2)}Ni_2)I)]^{3+}$	196(1) 195.2(0.6)			320 326		638 (in) 890 (out)	161.1
$[(L^{(2)}Ni_2)\ (ClO_4)]^{3+}$	193[o]					720 (in)	146.3
$[(L\ ^{(1)}Cu_2)Cl]^{3+}$[p]	197.3(0.5) (i) 201.0(0.55) (a)			254		508 (in)	
$[(L\ ^{(1)}Cu_2)Br]^{3+}$[p]	198 (i) 200 (a)			269		534 (in)	
$[(L\ ^{(1)}Ni_2)(ClO_4)]^{4+}$	189 (i) 193 (a)			p		705 (in)	
$[(L^{(b)}Ni)]Cl_2$[q]			206(1)		249		
$[(L^{(b)}Ni)]I_2$[r]	195(1)						

[a] Metal to macrocyclic ligand nitrogen distance(s), averaged over the four ring nitrogens (standard deviation in parentheses). Distances that are characteristic of low spin ($S = 0$ for Ni^{II}) macrocyclic ligand complexes are listed as $d_{M(l)-N}$; those characteristic of high spin are listed ($S = 1$ for Ni^{II}) as $d_{M(h)-N}$. [b] $L^{(1)}$ = α,α′-bis(5,7-dimethyl-1,4,8,11-tetraazacyclotetradeca-4,7-diene-6-yl)-*o*-xylene; $L^{(2)}$ = α,α′-bis(5,7-dimethyl-1,4,8,11-tetraazacyclotetradeca-6-yl)-*o*-xylene. Structural data reported in this work except as noted by references in parentheses. [c] Metal-bridging ligand distances. [d] Metal−metal distance within the $[L^{(n)}M_2]^{4+}$ moiety denoted as (in), between moieties as (out). [e] Reference 35. [f] Disordered, extreme positions are listed. The assignment of the spin state is ambiguous. [g] Bridge between tetrameric moieties, disordered, longest distance entered. [h] Bridge between dinickel moieties within a tetrameric unit. [i] Shortest Ni−Ni distance between dinickel moieties within a tetrameric unit. [j] Shortest Ni−Ni distance between tetrameric units. [k] This structure was determined at both 193 and 295 K; the structures were indistinguishable. [l] Perchlorate oxygen atom. [m] The bridging bromide within the dinickel complex is disordered; the average distance is listed. The assignment of the spin state is ambiguous. [n] Reference 34. [o] This is not a good quality structure (much disorder); a perchlorate is positioned between the macrocyclic ligand moieties of the dinickel complex. [p] No bridging ligand. [q] Reference 31. [r] Reference 32.

rings of this size,[64] and this is consistent with their observed diamagnetism.

Magnetic Properties. The magnetic data are summarized in Figure 8 and Table 4.

While the perchlorate salts and the iodide-bridged complexes have effective moments of $p_{eff} \approx 0.3\ \mu_B$, the chloride- and bromide-bridged complexes have effective moments of $p_{eff} \approx 3\ \mu_B$ per nickel complex above 50 K, where

$$p_{eff} = \sqrt{(3k_B T\chi_m/N_A{\mu_B}^2)} = 2.829\ \sqrt{(T\chi_m)} \qquad (4)$$

and k_B is Boltzmann's constant, χ_m is the magnetic susceptibility, N_A is Avogadro's number, and μ_B is the Bohr magneton. In addition, the effective moments for the bridged complexes have various temperature-dependent behaviors. The effective moment for the $[(L^{(2)}Ni_2)Cl(ClO_4)]^{2+}$ complex exhibits a smooth increase from 2.9 μ_B at 50 K to 3.0 μ_B at room temperature, while the $[(L^{(2)}Ni_2)Br(ClO_4)]^{2+}$ moment decreases from about 3.0 μ_B at 50 K to 2.9 μ_B at 270 K before a sudden 3% decrease in the moment over a 15 K temperature interval. In comparison, the moment for the dibromo complex closely follows the behavior of the monochloro complex up to 180 K before also exhibiting a sudden 3% decrease in the moment over a 15 K temperature interval. On the other hand, the tribromo complex has the largest effective moment (3.1 μ_B at 50 K), which gradually increases to 3.4 μ_B at the highest measuring temperature without any sudden changes in the moment. A very small temporal hysteresis (just beyond reproducibility resolution) between the ZFCM and the FCM was found below the temperatures at which the sudden changes in the effective moments occurred in these complexes (the FCM is slightly larger). Moreover, the sudden changes in magnetization are reproducible in separately prepared samples. Note that the X-ray studies indicate that there is a phase change in the dibromo complex structure between 100 and 300 K and the sudden changes in the effective moment may be correlated with this phase change. However, it is unlikely that a corresponding phase change occurs in the monobromo complex structure. Finally, we found no clear evidence for significant magnetic coupling between the nickel atoms within the bimetallic complexes ($|J| < 1\ cm^{-1}$).

The rapid decrease in the effective moment below 50 K found in all of the samples is consistent with previous work[34,35] and results from a zero-field (single-ion) splitting of the Ni^{II} ions.

Discussion

The xylene-linked, bis(metallo-macrocyclic ligand) complexes with metal−halide−metal bridges appear to be poised for strong, halide-mediated metal−metal coupling. Yet, the observations indicate that there is very little electronic coupling between the metals of the dinickel complexes described here or of the dicopper complexes described previously. Despite the lack of appreciable metal−metal coupling, the halide-bridged dinickel complexes display a wide structural variation. The range of structures exhibited by the dinickel complexes in which a bromide bridges the

(64) Curtis, N. F. In *Coordination Chemistry of Macrocyclic Compounds*; Melson, G. A., Ed.; Plenum: New York, 1979; p 219.

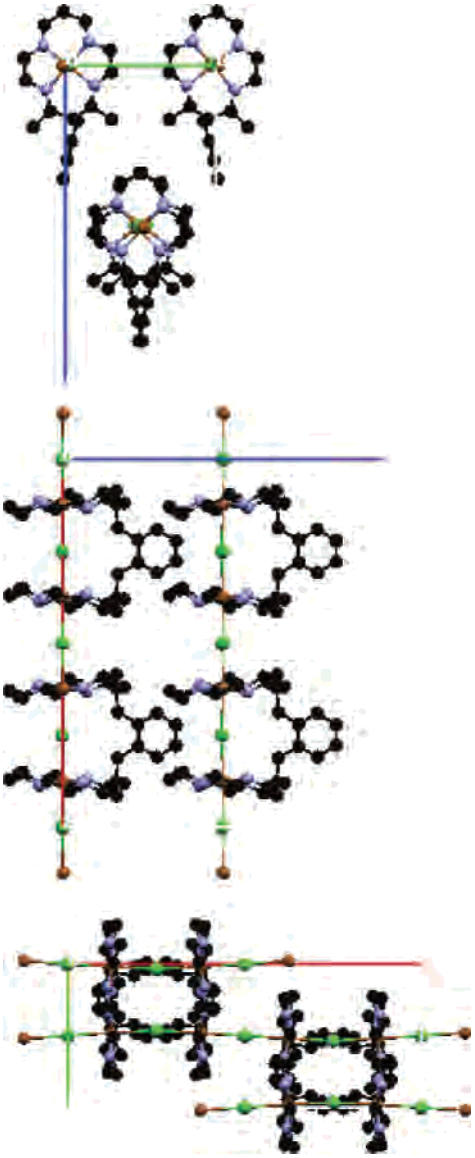

Figure 4. Views along the crystallographic *a* (red), *b* (green), and *c* (blue) axes (from top to bottom) for $[(L^{(2)}Ni_2)Br_2](ClO_4)_2$at 295 K.

two nickel centers in the complex are the most remarkable of the dinickel complexes examined, since each of these complexes is a mixed-configurational or electronic isomer containing one high-spin and one low-spin Ni^{II} center. Two of these complexes, $[(L^{(2)}Ni_2)(Br)_3]^+$ and $[(L^{(2)}Ni_2)(Br)_2]^{2+}$, even have different ambient and 100 K molecular structures. The structures of the dibromo complex are the most extraordinary since the high-temperature and low-temperature structures differ both in the localization of the electronic configurations of the Ni^{II} centers and in the large amplitude displacements of nickel-macrocyclic ligand moieties along infinite chains in the crystal lattice. The mixed-configurational dibromo and the tribromo dinickel complexes are the electronic configurational exchange analogues of mixed-valence complexes, such as the Creutz−Taube ion,[65,66] in electron-transfer systems. However, the dinickel complexes correspond to the weak coupling limit for configurational

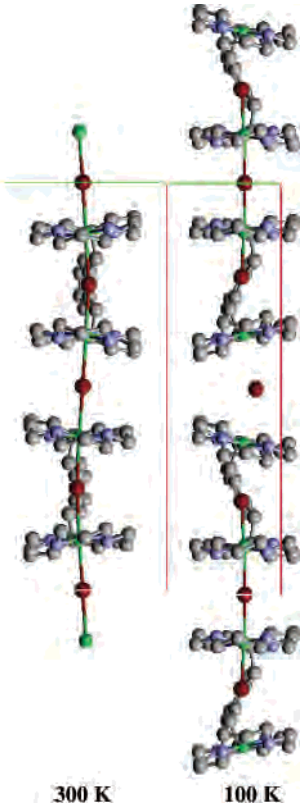

Figure 5. Comparison of the 300 K (left) and 100 K (right) molecular structures along single chains of $[L^{(2)}Ni_2Br_2]^{2+}$ moieties. Both structures are viewed along the unit cell *c*-axes (orthogonal to the infinite chains). Note that the unit cell volume of the 100 K structure is greater than that of the 295 K structure: the *b*-axis is nearly doubled and the *a*-axis is more than 1% longer at 100 K (see Table 2); the red lines in this figure are the distances between the centers of equivalent bromides of the structures. The Ni−Ni distances are compressed within the tetramers and lengthened between tetramers of the 100 K structure relative to those of the 300 K structure.

interchange in contrast to the strong coupling limit for electron transfer exemplified by the Creutz−Taube ion. Furthermore, the dipole−dipole coupling (or Förster) mechanism that is useful for most electronic excitation transfer processes[13,20,67,68] is not applicable to the ground-state processes of the systems described here; on the other hand, a molecular vibrational mode can mix the electronic configurations.

A. General Structural Features of the Dinickel Complexes. Nickel(II) complexes with aliphatic, 14-membered tetraazamacrocyclic ligands characteristically have equatorial Ni−N bond lengths that are significantly longer for the six-coordinate complexes in which the Ni^{II} centers have triplet spin multiplicity (typically 206 pm) than those for the planar, four-coordinate complexes in which the Ni^{II} centers have singlet multiplicities (typically 194 pm);[64] see Table 3. This standard correlation of the Ni^{II} electronic structure with coordination geometry fails with the dinickel complexes discussed here since the large electrostatic attractions favor the intercalation of an anion between the co-facial Ni^{II}-

(65) Creutz, C.; Taube, H. *J. Am. Chem. Soc.* **1969**, *91*, 3988.
(66) Creutz, C.; Sutin, N. *Inorg. Chem.* **1976**, *15*, 496.
(67) Yardley, J. T. *Introduction to Molecular Energy Transfer*; Academic: New York, 1980.
(68) Birks, J. B. *Photophysics of Aromatic Molecules*; Wiley-Interscience: New York, 1970.

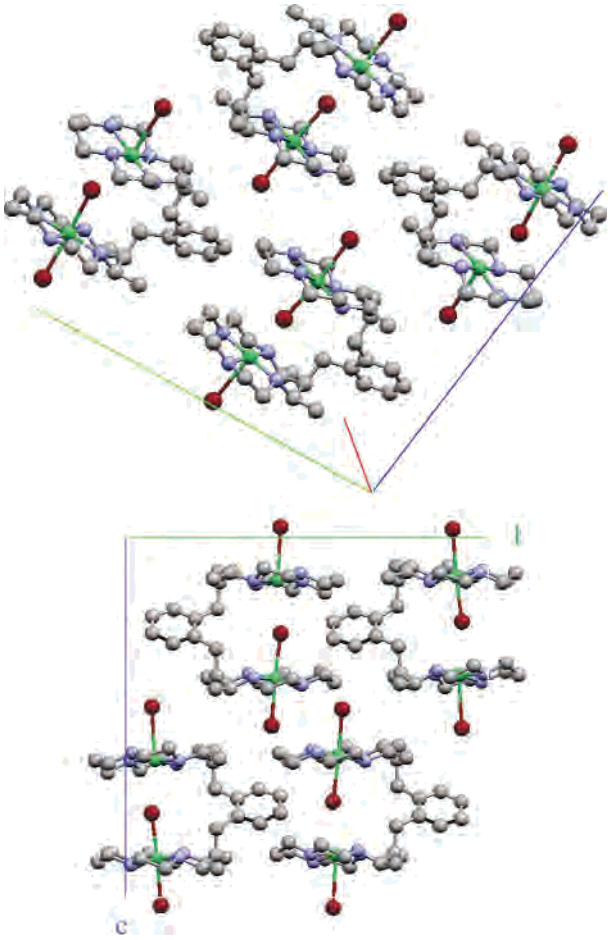

Figure 6. 100 K X-ray structure of $[L^{(2)}Ni_2Br_3]^+$ complex: packing, top; view along the crystallographic *a*-axis, bottom. The near sides of the phenyl rings are highlighted in the view at the bottom.

Figure 7. Molecular structure of $[L^{(1)}Ni_2]^{2+}$.

macrocyclic ligand moieties with the ion-pair association constants in excess of 10^4 M^{-1} and because the Ni−X_{axial} distances vary over a substantial range. The assignment of different coordination numbers to the different centers of a dinickel complex when there is a bridging anion would be arbitrary. Only for the diamagnetic $[L^{(1)}Ni_2]^{4+}$ complex have we found a clear example of a limiting Ni^{II} coordination geometry typical of mononickel-macrocyclic ligand complexes. The other diamagnetic complexes, $[L^{(2)}Ni_2I]^{3+}$ and $[L^{(2)}Ni_2(ClO_4)]^{3+}$, have intercalated anions and their Ni^{II} environments can be considered to be five-coordinate, but the $Ni^{II}-X^-$ interaction does not result in a high-spin ground-state electronic configuration at either metal center. In contrast, the monohalo complexes that intercalate a chloride

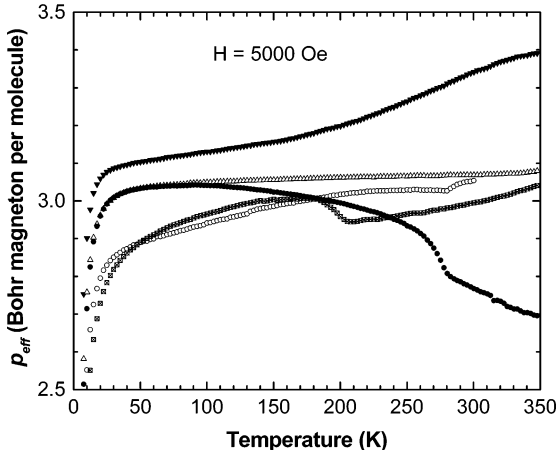

Figure 8. Temperature dependence of magnetic moment determinations for chloride- and bromide-bridged complexes: $[L^{(2)}Ni_2Cl(ClO_4)](ClO_4)_2$, △; $[L^{(b)}NiBr_2]$, ○ $[L^{(2)}Ni_2Br(ClO_4)](ClO_4)_2$, ●; $\{[L^{(2)}Ni_2Br_2](ClO_4)_2\}_n$, ■; $[L^{(2)}Ni_2Br_3](ClO_4)$ ▼.

Table 4. Summary of Magnetic Data on Tetraazamacrocyclic Ligand Complexes

complex	μ_{eff} (μ_B per M_n)
$\{[L^{(2)}Ni_2Cl_2)](ClO_4)_2\}_2$[a,b]	3.42 (100 K)
$[L^{(2)}Ni_2Cl(ClO_4)](ClO_4)_2$	2.94 (100 K)
$[L^{(2)}Ni_2Br(ClO_4)](ClO_4)_2$	3.02 (100 K)
$\{[L^{(2)}Ni_2Br_2](ClO_4)_2\}_n$	3.04 (100 K)
$[L^{(2)}Ni_2Br_3]Br$[c]	2.9 (100 K)
$[L^{(2)}Ni_2Br_3]ClO_4$	3.12 (100 K)
$[L^{(2)}Ni_2I](ClO_4)_3$	diamagnetic
$[L^{(2)}Ni_2(ClO_4)](ClO_4)_3$	diamagnetic
$[L^{(1)}Ni_2(ClO_4)](ClO_4)_3$	diamagnetic
$[L^{(1)}Cu_2Cl](ClO_4)_3$[d]	2.48
$[L^{(1)}Cu_2Br](PF_6)_3$[d]	2.12
$[L^{(b)}Ni](Br)_2$	3.05 (100 K)
$[L^{(b)}Ni](I)_2$[e]	diamagnetic

[a] For this complex, the exchange interaction through bridging ligands within the $[M_2L^{(n)}]^{4+}$ moiety, $J_{intra} = -11.2$ cm^{-1}, and the exchange interaction through ligands between moieties, $J_{inter} = -48.2$ cm^{-1}.[35] For the other complexes, the exchange interaction energies are less than 1 cm^{-1}. [b] Reference 35. [c] Reference 34. [d] Reference 54. [e] Reference 32.

or a bromide ion between the Ni^{II} centers of $[L^{(2)}Ni_2]^{2+}$ result in a single, structurally well-defined high-spin Ni^{II} center that becomes six-coordinate by capturing one of the perchlorate anions, a single low-spin Ni^{II} center with the expected equatorial Ni−N bond lengths, and a measured magnetic moment which is characteristic of a single triplet state per dinickel complex over the temperature range of 5−325 K (Figure 8). These complexes have a mixed-electronic configuration in their ground states, $\{^3Ni^{II},^1Ni'^{II}\}$, and since their coordination spheres are so dissimilar, the other electronic isomer, $\{^1Ni^{II},^3Ni'^{II}\}$, is an electronic excited state. Since the thermal population of this excited state would not affect the observed magnetic properties, we have no experimental estimate of its energy. Furthermore, these salts contain an excess of perchlorate anions, so that the observation of one high-spin and one low-spin center in the chloride- and bromide-bridged complexes is a demonstration that these halides do not simultaneously form covalent linkages to both metals in these complexes. Several issues that are raised by these observations are elaborated below.

Figure 8 shows that the actual magnetic behavior of the monochloro and monobromo complexes is somewhat more

complicated than the previous paragraph suggests. We attribute these complexities to relatively small energies of excited states with different electronic configurations and spin multiplicities. Thus, the relatively shallow increase of magnetic moment observed for the $[L^{(2)}Ni_2Cl(ClO_4)]^{2+}$ complex above $T = 50$ K can be attributed to the thermal population of relatively low-energy excited states with the $\{^3Ni^{II},^3Ni'^{II}\}$ ($\sim$500 cm^{-1}; see Supporting Information)[69] and the $\{^1Ni^{II},^1Ni'^{II}\}$ ($\sim$270 cm^{-1}) electronic configurations; the shallow decrease of magnetic moment observed for the $[L^{(2)}Ni_2Br(ClO_4)]^{2+}$ complex above $T = 50$ K can be attributed to the much higher energy of the $\{^3Ni^{II},^3Ni'^{II}\}$ configuration when bromide is the bridging ligand. This inferred contrast in the energies of the $\{^3Ni^{II},^3Ni'^{II}\}$ electronic configuration in these two complexes is also more consistent with the much larger bridging-ligand-mediated $^3Ni^{II}/^3Ni^{II}$ coupling reported[35] for chloride than we find for bromide. In any case, the observed magnetic behavior of these complexes implies that the zero-point energy differences between their different singlet and triplet electronic configurations are very small. This implies that relatively small changes in the positions of the axial ligands could effect an inversion of the triplet and singlet energies at the Ni^{II} centers of the dinickel complexes.

While the magnetic measurements of the dibromo- and tribromo-dinickel complexes indicate that they also have one triplet center per dinickel complex, the Ni^{II} centers of these complexes have coordination environments that are indistinguishable at 300 K, but while their coordination numbers and magnetic moments are largely unchanged at 100 K, their bond lengths are those characteristic of one high-spin and one low-spin Ni^{II} center. These similar coordination environments suggest that the vibrationally equilibrated $\{^3Ni^{II},^1Ni'^{II}\}$ and $\{^1Ni^{II},^3Ni'^{II}\}$ electronic configurations must have nearly the same zero-point energies. Thus, the ambient structures of the di- and tribromo complexes appear to be the consequence of the thermally promoted fluctuation of the high- and low-spin electronic configurations. This interconfigurational exchange may be represented as (the prime is used to distinguish the different Ni^{II} ions)

$$[(L^{(2)}\{^3Ni^{II},^1Ni'^{II}\})Br_3]^+ \rightleftarrows [(L^{(2)}\{^1Ni^{II},^3Ni'^{II}\})Br_3]^+ \quad (5)$$

The $^3Ni/^1Ni$ exchange between the nearly identical metal centers can be described as a triplet excitation transfer process near to the limit of zero energy difference between the initial and final electronic configurations. This is the excitation energy analogue of intervalence electron transfer in mixed-valence systems. Thus, these complexes are clearly unique systems, and several aspects of their properties are considered below.

B. Implications of the Structural and Magnetic Studies for Models of Ligand-Mediated Electronic Configurational Exchange. In our studies of the solution behavior of these complexes,[56] we were unable to find evidence for the $\{Ni^{II},Ni^{II}\} \rightarrow \{Ni^{I},Ni^{III}\}$ metal-to-metal charge-transfer absorption that is expected to accompany strong metal−metal coupling.[14,15,50] The solid-state studies reported here demonstrate that the halide-mediated metal−metal coupling is very weak in these complexes and that their magnetic properties are somewhat complicated by the thermal population of low-energy excited states. Since these are axially labile metal complexes, the variations in their structures and magnetic properties must reflect a balance between (a) crystal packing forces, (b) stereochemical and electrostatic repulsions between the cationic complexes, (c) electrostatic attractions between the cations and anions, (d) electrostatic repulsions between the anions and electrons in the $d\sigma_\perp$ orbitals (orthogonal to the N_4 plane of the macrocyclic ligands), and (e) covalent bonding between the metals and the axial ligands. The gross contrasts between the 300 and 100 K structures of $\{[L^{(2)}Ni_2Br_2](ClO_4)_2\}_n$ demonstrate that crystal-packing forces do play a role in determining the structures. While the last three classes of interactions (c−e) fall into the regime of effects treated theoretically with standard ligand-field models for vertical transitions between electronic states of the same spin multiplicity in complexes in which the Ni−X bond distances are constant for a given halide ligand,[70,71] the observations in this report relate to the zero-point energy differences between the electronic states in which the individual metal centers differ in spin multiplicity in bimetallic complexes with an appreciable range of Ni−Br distances. Since the magnetic measurements indicate that the relevant energies are very small, less than 10^3 cm^{-1}, they are unlikely to be adequately treated by an attempt to adjust the ligand-field parameters for variations in Ni−Br distances[70,71] for the effect of cationic charge on the ligand-field strength of the bridging halide, for the differences in spin multiplicity, and/or for the shapes of the potential energy surfaces. The approximate energies inferred from temperature-dependent magnetic behavior and a simple model of the equilibrium populations of states of different spin multiplicities are sufficient to illustrate the issues raised by this study.

1. Correlation of Electronic Structure with Metal Ligand Bond Lengths. The molecular structures of the monohalo complexes can be taken as a reference for the coordination-sphere bond lengths that are characteristic of high-spin and low-spin Ni^{II} centers in this series of complexes. The tribromo- and the dibromo dinickel complexes both have one high-spin and have one low-spin center, but the ambient molecular structures have bond lengths that are the average for those electronic configurations. Since the structure of $[L^{(2)}Ni_2Br_3]^+$ contains individual molecules, it is the simplest focus for discussion. The 100 K structure shows one high-spin Ni(II), with long Ni−N (207 pm) and short Ni−Br bonds (262 and 271 pm, inside and outside the dimer, respectively), and one low-spin Ni(II), with short Ni−N (196 pm) and long Ni−Br (332 and 307 pm) bonds. It is also noteworthy that both of the external axial Ni−Br distances differ by 18 pm in the two structures, one larger

(69) Supporting Information, see paragraph at the end of this paper.

(70) Lever, A. B. P. *Inorganic Electronic Spectroscopy*; Elsevier: Amsterdam, The Netherlands, 1984.

(71) Figgis, B. N.; Hitchman, M. A. *Ligand Field Theory and Its Applications*; Wiley−VCH: New York, 2000.

and the other smaller in the ambient structure, but without evidence of the disorder exhibited by the bridging bromide. Since the conversion of a triplet Ni^{II} center to a singlet center results when the axial bond lengths increase and/or the equatorial bond lengths decrease, the interchange of electronic configurations and the interchange of the coordination-sphere bond lengths are inseparable processes of the Ni(II) centers, and the change of electronic configurations must be coupled to one or more vibrational modes of the complex. This concerted electronic/nuclear interchange process can be described in terms of the changes in potential energy of the different electronic configurations, $[(L^{(2)}\{^3Ni^{II},{}^1Ni'^{II}\})Br_3]^+$, $[(L^{(2)}\{^1Ni^{II},{}^3Ni'^{II}\})Br_3]^+$, and $[(L^{(2)}\{^3Ni^{II},{}^3Ni'^{II}\})Br_3]^+$, with activation of the correlated vibrational modes, and it is qualitatively illustrated in Figure 9 for different energies of the $[(L^{(2)}\{^3Ni^{II},{}^3Ni'^{II}\})Br_3]^+$ configuration relative to the energy of the degenerate $[(L^{(2)}\{^3Ni^{II},{}^1Ni'^{II}\})Br_3]^+$ and $[(L^{(2)}\{^1Ni^{II},{}^3Ni'^{II}\})Br_3]^+$ configurations in the region of the intersection of their diabatic PE surfaces. Since the Ni−Ni distance is the same at 100 and 300 K, the correlated nuclear motions can be simply described as an antisymmetric (with respect to a C_2 symmetry axis that is orthogonal to the Ni−Ni axis) combination of the motions of the atoms coordinated to the two Ni centers. These ligand motions at each metal are similar to one of the degenerate the e_g-skeletal vibrations (Q_θ) of an octahedral complex, but the bridging bromide must move in a concerted manner between the two Ni^{II} centers, and this is different from the thermal fluctuations characteristic of Jahn−Teller vibronic coupling at a single metal center.[72,73]

2. Some Considerations Regarding the Singlet−Triplet Zero Point Energy Differences. Each Ni^{II} center of the dimer has a singlet ground state when the axial coordination is weak or absent. The triplet excited state generated from a four-coordinate-planar Ni^{II} complex is necessarily vibrationally excited unless there are changes of coordination number and equatorial bond lengths; see Figure 2. Such a triplet state is the Franck−Condon excited state generated by light absorption (vertical energy E_{ST}). The thermally generated triplet Ni^{II} center in such a complex has the thermally equilibrated, vibrationally relaxed, coordination geometry (zero-point energy $E_{ST}{}^{00'}$). The experimental observation that Ni/Ni electronic coupling is very weak in these complexes suggests that (a) we can neglect electronic coupling between Ni^{II} centers in the ground state, (b) the excited states of the dinickel complexes which have ferro- and antiferromagnetically coupled triplet states differ little in energy, and (c) the complexes in which the Ni^{II} centers have the same spin multiplicity are low-energy electronic excited states.

All of the $L^{(1)}Ni_2$ complexes have singlet spin multiplicity in solution, and the association of the complexes with anions in solution shifts the 21 000 cm^{-1} ligand-field absorption band of the parent to slightly lower energies in the 1:1 ion

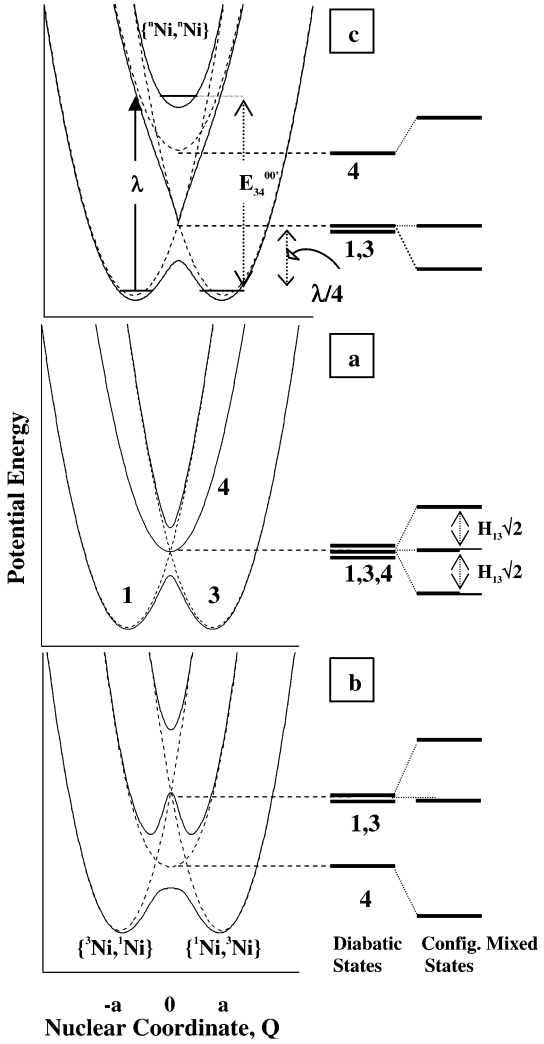

Figure 9. Qualitative PE diagrams illustrating the effects of configurational mixing between the $S = 1$ component of a $[(L^{(2)}\{^3Ni^{II},{}^3Ni^{II}\})XY_2]$ excited state (**4**) on the energies of degenerate $[(L^{(2)}\{^3Ni^{II},{}^1Ni^{II}\})XY_2]^{2+}$ (**1**) and $[(L^{(2)}\{^1Ni^{II},{}^3Ni^{II}\})XY_2]^{2+}$ (**3**) ground-state electronic configurations; see Scheme 1. In the diabatic limit (no configurational mixing and no metal−metal coupling), the $[(L^{(2)}\{^3Ni^{II},{}^3Ni^{II}\})XY_2]^{2+}$ (M_S = 1, 3, and 5) and $[(L^{(2)}\{^1Ni^{II},{}^1Ni^{II}\})XY_2]$ excited states are degenerate with an energy of approximately $\lambda/4$, a. If there is significant $^3Ni-X-{}^3Ni$ three-center covalent bonding in the electronic configuration **4**, then the energies of the diabatic states with configuration **4** are smaller than $\lambda/4$, b. The energy of the PE minimum of the diabatic $[(L^{(2)}\{^3Ni^{II},{}^3Ni^{II}\})XY_2]$ configuration may also be greater than $\lambda/4$, c. The adiabatic ground-state curves are constructed assuming that there is no mixing between the ground state configurations and that only the $M_S = 3$ component with the $[(L^{(2)}\{^3Ni^{II},{}^3Ni^{II}\})XY_2]^{2+}$ electronic configuration will mix with the two ground-state configurations. For simplicity, the only excited states included in these diagrams are for configuration **4** with $M_S = 3$; the vibrational levels are omitted (except for the 0th levels in the top diagram). The adiabatic curves correspond to the functions V_+ (in eq 19), V_a (in eq 15), and V_- (in eq 19) from top to bottom, respectively.

pairs.[56] Thus, the electrostatic contributions to Ni−X bonding may be similar from one halide to another, and the different halides do not result in different magnetic properties of these complexes. In contrast, different halides result in different magnetic properties of the $L^{(2)}Ni_2$ complexes. The different effects of the axial ligands on the magnetic properties of the complexes can be attributed to small energy differences in the covalent components of the different Ni−X bonds. A simple linear combination of the relevant atomic orbitals

(72) Riley, M. J.; Hitchman, M. A.; Mohammed, A. W. *J. Chem. Phys.* **1987**, *87*, 3766.
(73) Simmons, C. J.; Stratemeier, H.; Hanson, G. R.; Hitchman, M. A. *Inorg. Chem.* **2005**, *44*, 2753.

description (or to an equivalent angular overlap model argument) is adequate for our purposes. The weak axial covalent contributions for a single Ni^{II} complex can be represented in terms of the symmetric combinations of one p_σ orbital from each axial ligand with the metal $3d_\sigma$ orbitals (for simplicity in this discussion, we neglect the antisymmetric combinations of ligand p_σ with the metal $4p_\sigma$). A covalent contribution requires partially occupied axial d_σ orbitals of the Ni^{II} triplet state. It is convenient to separate the two axial bonding contributions so that the energy of the axial bond is $[\epsilon(\sigma_X) + \epsilon(\sigma_Y)]$, for the axial ligands X and Y. If the Ni centers in the ion pairs have singlet ground states, then $E_{ST}°$ is a promotion energy for bond formation in an ion-pair complex (i.e., the "square-planar" triplet state is generated so that all of the coordinates except the axial Ni−X coordinates have their equilibrium triplet state values; thus, $E_{ST}°$ also contains a number of contributions including the electrostatic perturbation of the d_σ orbital, the differences in equatorial bond strength in the two states, and the electronic pairing energy). Then the energy difference between the singlet and triplet states is

$$E_{ST}^{00'} \cong E_{ST}° - [\epsilon(\sigma_X) + \epsilon(\sigma_Y)] \qquad (6)$$

Equation 6 expresses the concept that a five- or six-coordinate complex of triplet spin multiplicity will form only if the covalent contribution to the axial bond energy exceeds the singlet−triplet promotion energy in the correlated ion pair. The dihalide, monometallic complexes of Ni^{II} with the 14-membered macrocyclic-tetraamine ligands have triplet ground states for all of the halides except iodide.[70] This indicates that the Ni−I covalent bond energy contribution is smaller than the $E_{ST}^{00'}$value. In solutions of donor solvents (e.g., water, DMF, or acetonitrile), the $[L^{(2)}Ni_2]^{4+}$ complex is a mixture of singlet and triplet state configurations.[56] This suggests that the $E_{ST}°$ value is small.

3. Three-Center Bonding Contributions. Neglecting any differences in stereochemical constraints, and for a weak axial metal-halide bond with an energy $\epsilon(\sigma_X)$, the energy contribution of the three-center bond at each Ni center is approximately $^1/_2\epsilon(\sigma_X)$ so that eq 6 becomes

$$E_{ST}^{00'} \cong E_{ST}° - [^1/_2\epsilon(\sigma_X) + \epsilon(\sigma_Y)] \qquad (7)$$

Equations 6 and 7 suggest that only one Ni center of a trihalide complex will have triplet spin multiplicity if the bridging halide−nickel bond energy $\epsilon(\sigma_X)$ is not much different from $E_{ST}°$, so that $[^1/_2\epsilon(\sigma_X) + \epsilon(\sigma_Y)] < E_{ST}° < [\epsilon(\sigma_X) + \epsilon(\sigma_Y)]$, and that both centers will have triplet spin multiplicity only if $[^1/_2\epsilon(\sigma_X) + \epsilon(\sigma_Y)] > E_{ST}°$. Only in the $\{[\{L^{(2)}Ni_2\}Cl_2]\}_2^{4+}$ tetramer is there evidence for significantly more than one paramagnetic Ni center per dinickel complex.[35] This, and the diamagnetism of the $[L^{(2)}Ni_2I]^{3+}$ complex, suggests a systematic decrease in $\epsilon(\sigma_X)$ from chloride to iodide, that is, a classical sequence of bond energies.

C. Idealized Models for Electronic Excitation Energy Transfer. The tribromo complex is relatively simple, but its structures exhibit the most interesting and puzzling features that are found in this family of complexes: (i) one paramagnetic Ni center per dinickel moiety, (ii) different ambient and 100 K structures, and (iii) similar coordination environments of both Ni centers in the ambient structure. In this section, we propose a relatively simple vibronic model to account for these features.

Scheme 1. Different Ni(II) Electronic Configurations in the Dinickel Complexes.

$[L^{(2)}(^3Ni,{}^1Ni')Br_3]^+$	⇄	$[L^{(2)}(^1Ni,{}^1Ni')Br_3]^+$
$\{d\sigma_{//}\, d\sigma_\perp, d\sigma_\perp'^2\}$		$\{d\sigma_\perp^2, d\sigma_\perp'^2\}$
(**1**)		(**2**)
⇅		⇅
$[L^{(2)}(^3Ni,{}^3Ni')Br_3]^+$	⇄	$[L^{(2)}(^1Ni,{}^3Ni')Br_3]^+$
$\{d\sigma_{//}\, d\sigma_\perp, d\sigma_{//}'d\sigma_\perp'\}$		$\{d\sigma_\perp^2, d\sigma_{//}'d\sigma_\perp'\}$
(**4**)		(**3**)

1. Limit in Which the Metal Centers are Electronically Independent. This limit corresponds to an isolated ion (in vacuo) in which the singlet and triplet states of each metal can be independently populated. Ligand-field theory arguments are in principle only applicable in this limit. However, the singlet−triplet transition at one center requires the motion of a bridging halide between the metal centers, and this motion is necessarily coupled to the change of electronic configuration at the other metal center. This point is illustrated below by first assuming that the two metal centers are independent and then showing that this assumption is not consistent with the properties of these complexes.

If the singlet and triplet configurations of each metal in Scheme 1 below are populated one at a time, then four different electronic configurations (or orbital populations) will result because the complex contains two different metals (the prime is used to distinguish the different Ni^{II} ions).

The orbital populations of the two highest energy d-orbitals of the Ni^{II} centers are indicated in braces for each electronic configuration in Scheme 1, with the orbital in the N_4 plane of the macrocyclic ligand designated as $\mathbf{d}\sigma_{||}$ and the orbital orthogonal to this plane as $\mathbf{d}\sigma_\perp$.

Configurations **1** and **3** correspond to different, but chemically indistinguishable, electronic states of the complex; thus, we assume a limit in which these states have the same zero-point energies, $E_1° = E_3^{0'}$ and $E_{13}^{00'} = 0$. Furthermore, each of these four different electronic configurations of the complex must have a unique set of equilibrium nuclear coordinates in order for the electronic states to be independent of one another. For simplicity, we assume that the diabatic (*d*) potential energy (PE) of the *i*th electronic state can be adequately represented as simple harmonic oscillator (sho) displacements in the nuclear coordinates of the atoms around the individual Ni centers

$$PE_{i(d)} \cong E_i^0 + \sum_X \frac{f_{NiX}^i}{2} Q_{NiX}^{i\,2} + \sum_Y \frac{f_{Ni'Y}^i}{2} Q_{Ni'Y}^{i\,2} \qquad (8)$$

The sum is over all of the Ni−X and Ni′−Y bond distances and angles, where E_i^0 is the zero point energy of the *i*th state, the f^k_{NiZ} values are local (i.e., bond not normal mode) force constants, and Q^i_{NiZ} is the difference in the Ni−Z bond length and its equilibrium value at the PE minimum. In the simplest case, the electronic states would have the same force constants with ΔQ_{NiZ} being the difference in Ni−Z bond lengths evaluated at the two PE minima. A necessary consequence of the tribromo-complex structure is that the bridging bromide is part of a unique nuclear coordinate in the actual tribromo complex, since its motion is between Ni and Ni′. If the distance between the PE minima of **1** and **3** along this coordinate is (*a* in Figure 9a) $\Delta Q^{00'}_{3_{\mathrm{Ni}}} = (Q^0_{3_{\mathrm{Ni}}} - Q^{0'}_{3_{\mathrm{Ni}}}) = 2a$ and $x =$ the amplitude of the displacement along this coordinate, $0 \le x \le 2a$, then

$$\Delta Q_{\mathrm{NiBr}} = x \qquad \text{and} \qquad \Delta Q_{\mathrm{Ni'Br}} = 2a - x \tag{9}$$

Therefore, the respective nuclear coordinates of the two Ni^{II} ions are coupled, and the electronic states cannot be independent. As a consequence, the matrix element that mixes the electronic configurations **1** and **3** is $H_{13} = (bQ_c + H_{13}^{\circ})$ where *b* is a constant, Q_c, the displacement of the coupled vibration (chosen so that $Q_c = 0$ when $x = {}^1/_2\Delta Q^{00'}_{3_{\mathrm{Ni}}}$), and H_{13}°, the nuclear coordinate-independent coupling matrix element. Even for $H_{13}^{\circ} = 0$, the coordinate dependence of H_{13} is sufficient to mix the electronic configurations.

2. Concerning the Electronic Coupling between the Degenerate Electronic Configurations 1 and 3. Since the susceptibility results indicate that the magnetic coupling between Ni^{II} centers is very small at the ground-state PE minima, the magnetic exchange energy for a three center bonding model given by $J \cong 2H_{13}^2/E_{13}$ will be less than 1 cm^{-1}.[74] If the electronic coupling between Ni^{II} centers is very weak for all of the electronic configurations and for all of the values of Q_c, then the three states are degenerate at the diabatic crossing point, $Q_c = 0$ (Figure 9a). The energy of the diabatic crossing of these states, $\lambda/4$, can be estimated to be about 560 cm^{-1} from the fitting of the high-temperature magnetic moment of $[L^{(2)}Ni_2Br_3]^+$, so that $E_{13} \cong \lambda \approx 2200$ cm^{-1} (sho limit) and the electronic-coupling matrix element $H_{13}^{\circ} < 33$ cm^{-1}. Any configurational mixing between the electronic configurations **1**, **3**, and **4** will result in a larger value of H_{13} at the diabatic crossing point even for very weak electronic coupling between the ground-state configurations **1** and **3**. There are three degenerate states of configuration **4** which differ in spin multiplicity ($M_S = 2S + 1$, $S = 0$, 1, or 2). The electronic state of configuration **4** for which $M_S = 3$ can mix with triplet configurations **1** and **3** to reduce the barrier to configurational interchange. Any configurational mixing will be largest at $Q_c = 0$ since all three of the states are degenerate at this point; see Figure 9a. The increase of the magnetic moment observed for $[L^{(2)}Ni_2Br_3]^+$ with increasing temperature must be attributed to the thermal population of an electronic excited state with $M_S = 5$, and since this state will not mix with the triplet configurations, its energy is a measure of the energy of the diabatic crossing point in the very weak coupling limit.

3. Vibronic Coupling of the Ni(II) Electronic Configurations in $[L^{(2)}Ni_2Br_3]^+$ in the Weak Coupling Limit. The electronic configuration of each Ni^{II} center depends on its coordination. If we assume the average of the high-spin and low-spin Ni-ligand bond lengths as a reference ($Q_c = 0$ in Figure 9), then the molecular structure of $[L(^3Ni,{}^1Ni')Br_3]^+$ can be represented as $(\delta_{\parallel}{}^+\delta_{\perp}{}^-,\delta_{\parallel}{}'^-\delta_{\perp}{}'^+)$, where $\delta_{//}$ and $\delta_{\perp}$, respectively, represent the nuclear displacements of ligands within and orthogonal to the N_4 plane of the MCL ligand and "+" and "−" designate expansions or contractions of the coordination-sphere bond distances (relative to $Q_c = 0$). For simplicity, we designate this set of nuclear coordinates as $(\delta_{\parallel}{}^+\delta_{\perp}{}^-,\delta_{\parallel}{}'^-\delta_{\perp}{}'^+) = \{Q_{\theta(+)},Q_{\theta(-)}\}$. Then, the process in eq 5 is coupled to the molecular vibration that correlates with the changes of orbital occupation. The correlated vibration may be represented as

$$\{Q_{\theta(+)},Q_{\theta(-)}\} \rightleftarrows \{Q_{\theta(-)},Q_{\theta(+)}\} \tag{10}$$

As noted in the preceding discussion, this is a molecular vibration and not the sum of the independent vibrations of two independent Ni^{II} centers. This vibration is the principle nuclear coordinate involved in the interchange of electronic configurations **1** and **3** as represented in Figure 9. This vibrational mode itself is sufficient to mix the electronic configurations **1** and **3**, and this is illustrated by the idealized model sketched below.[69]

It is initially useful to consider an isolated mononickel complex with (a) two axial bromides at large distances (as in an ion pair) and singlet spin multiplicity, (b) a vertical energy of E^d_{ST} for the triplet excited state, (c) the displacement $Q_{\theta(\mathrm{L})}$ in a single relevant vibrational mode that correlates with the energy difference, E_{ST}, between the $^1Ni^{II}$ and $^3Ni^{II}$ electronic configurations, and (d) a linear vibronic constant *b*. For simplicity, we use a coordinate system such that $E_{\mathrm{ST}} = 0$ for $Q_{(\mathrm{L})} = {}^1/_2\Delta Q^{00'}_{3_{\mathrm{Ni}}}$ and the PE minimum for $Q_{(\mathrm{L})} = a$. Then for this single metal center with E^d_{ST} large and in the sho limit

$$\mathrm{PE}_{\mathrm{L}(\pm)} = {}^1/_2 f(Q_{(\mathrm{L})} - a)^2 + \epsilon_{\pm} \tag{11}$$

where

$$\epsilon_{\pm} = {}^1/_2 E^d_{\mathrm{ST}} \pm {}^1/_2[(E^d_{\mathrm{ST}})^2 + 4b^2(Q_{(\mathrm{L})} - a)^2]^{1/2} \tag{12}$$

The resulting PE functions describe curves qualitatively analogous to those in Figure 2 (near to their PE minima) but with an allowed crossing in the region of their intersection at the value of $Q_{(\mathrm{L})}$ for which $E_{\mathrm{ST}} = E_S - E_T = 0$. The differences in force constants and PE minima of the singlet and triplet PE functions are neglected for simplicity and used to emphasize the dependence of the electronic configurations on the correlated nuclear coordinate.

For a complex with *two* equivalent Ni(II) centers, the electronic configuration of each center in the independent complex metal center limit can be described by similar

(74) Udugala-Ganehenege, M. Y.; Heeg, M. J.; Hyhroczuk, L. M.; Wenger, L. E.; Endicott, J. F. *Inorg. Chem.* **2001**, *40*, 1614.

secular equations that differ in their distortion coordinates, $Q_{\theta(L)}$ and $Q_{\theta(R)}$. The motion of the bridging ligand couples these distortion coordinates if this coupling is very weak $b'Q_c \ll bQ_{\theta(L)}$ (b is a linear coupling coefficient for the electronic states of a single metal center and b' is used for the coupling between the electronic states of different metal centers). The resulting system, in the Q_c coordinate defined above can be represented by

$$\begin{vmatrix} |PE_{L(\pm)}| - \epsilon & b'Q_c \\ b'Q_c & |PE_{R(\pm)}| - \epsilon \end{vmatrix} = 0 \qquad (13)$$

The coordinate Q_c is related to x in eq 9, but it is symmetrical with respect to the two metals, and this is usually the better choice for use in eq 13. As a consequence, this motion results in coupling of the coordination-sphere vibrational modes, so that $Q_{\theta(S)} = Q_{\theta(L)} + Q_{\theta(R)}$ and $Q_{\theta(A)} = Q_{\theta(L)} - Q_{\theta(R)}$, where the displacement in $Q_{\theta(S)}$ can be represented by

$$\{Q_{\theta(+)}, Q_{\theta(+)}\} \rightleftarrows \{Q_{\theta(-)}, Q_{\theta(-)}\} \qquad (14)$$

Similarly, eq 10 represents $Q_{\theta(A)}$. When both metals in the bimetallic complex have the same spin multiplicity the solutions of eq 14 are of the form

$$V_a = PE_{a(d)} + |b'q| \qquad (15)$$

and

$$V_b = PE_{b(d)} - |b'q| \qquad (16)$$

Since the approximate fitting of the magnetic susceptibility data suggests that the electronic state for configuration **2** may be slightly lower in energy than that for configuration **4** (energies of approximately 520 and 560 cm^{-1}, respectively), we identify V_b with **2** and V_a with **4**.

When the two metals have different spin multiplicities, their interchange is coupled to the distortion coordinate $Q_{\theta(A)}$, but it is now necessary to take account of the energies of the singlet and triplet states at each metal. The vertical energy differences between the ith and jth electronic states can be represented as

$$E_{ST(i)} = E_{ST(i)}{}^{00'} + \lambda_i \qquad (17)$$

where the reorganizational energy, λ_I, for the single vibrational mode in the sho limit is of the form

$$\lambda_i \approx \frac{f_\theta(Q^0_{3_{Ni}} - Q^0_{1_{Ni}})^2}{2} \approx \frac{f_\theta(\Delta Q^{00'}_{3_{Ni}})^2}{2} = 2f_\theta a^2 \qquad (18)$$

For the diabatic PE minima at $Q_c = \pm a$, the solutions of the secular equation in the sho limit can be expressed as

$$V_\pm \cong \frac{\lambda}{4}\left[\left(\frac{Q_c}{a}\right)^2 + 1\right] \pm \left|\frac{Q_c}{a}\right|[\lambda^2 + b'^2a^2]^{1/2} \qquad (19)$$

The PE function $V_\pm$ describes the configurational interchange of eq 5 with a single PE surface in a purely vibronic coupling limit ($H_{13}^\circ = 0$). The treatment described here is closely related to vibronic models described elsewhere.[72,75,76] The behavior of the functions V_a, V_b, and $V_\pm$ is qualitatively illustrated in Figure 9a. Strong vibronic coupling (i.e., a relatively large value of b') or configurational mixing between the $M_S = 3$ state of configuration **4** and configurations **1** and **3** will lower the PE barrier between the two degenerate ground-state configurations. The fitting of the magnetic data implies that the diabatic barrier is only $\lambda/4 \leq 520$ cm^{-1} (assuming that all of the diabatic configurations are degenerate for $Q_c = 0$), and if vibronic and/or configurational mixing were to reduce it to less than about 200 cm^{-1}, then there would be no effective barrier to the interchange under ambient conditions and the stationary state values of the nuclear coordinates contributing to the adiabatic PE would be approximately the average of the coordinates for the triplet and singlet states of the equivalent isolated Ni(II) complex. Thus, the vibronic approach provides a mechanism for the averaging of the nuclear coordinates in the ambient structures of the dibromo and the tribromo complexes that appears to be more consistent with the observations than the alternative of disordered electronic isomers in the ambient structures.

4. Other Mechanisms for Electronic Configurational Interchange. The interchange of electronic configurations **1** and **3** will be facilitated when the energy of **4** is less than $\lambda/4$ (i.e., for $E_{ST} \neq 0$ when $Q_c = 0$ or if three-center bonding is relatively significant in configuration **4**). When this is the case, $E_4{}^0(Q_c = 0) < E_k\ (Q_c = 0)$ (k = **1** or **3**), and this is illustrated in Figure 9b.

The remaining possibility, $E_4{}^0(Q_c = 0) > E_{1,3}\ (Q_c = 0)$, is illustrated in Figure 9c. Configurational mixing in this limit is analogous to that used to describe superexchange coupling in electron-transfer systems,[14,15,50] but it seems relatively unlikely here since some bridging-bromide-mediated coupling (as in weak three center bonding) of the $^3Ni^{II}$ centers in configuration **4** of the dinickel complex is more likely than bromide-mediated repulsion.

5. Other Features of the Halide-Bridged Dinickel Complexes. The axial ligand bond lengths in structures with well-defined high-spin and low-spin coordination sites vary more than is observed in mononickel complexes. For example, the external ^3Ni-Br bond is 8 pm longer and the ^1Ni-Br bond is 25 pm smaller than the corresponding bridging Ni−Br bonds in the $[L^{(2)}Ni_2Br_3]^+$ structure at 100 K. This must be a consequence of the different environments of the two halides, and it can be qualitatively addressed by considering the opposing contributions from (a) electrostatic interactions (attractions between the cations and anions and repulsions between the cations), (b) covalent interactions, and (c) electronic repulsions between the axial metal electrons and the electrons of the halide. The first of these contributions will be smaller for the bridging halide than for the external halide since the component of the electrostatic field along the Ni−Ni axis will be nearly independent of

(75) Ballhausen, C. J. In *Vibronic Processes in Inorganic Chemistry*; Flint, C. D., Ed.; Kluwer: Dordrecht, The Netherlands, 1989; p 53.
(76) Bersuker, I. B. *The Jahn−Teller Effect and Vibronic Interactions in Modern Chemistry*; Plenum: New York, 1984.

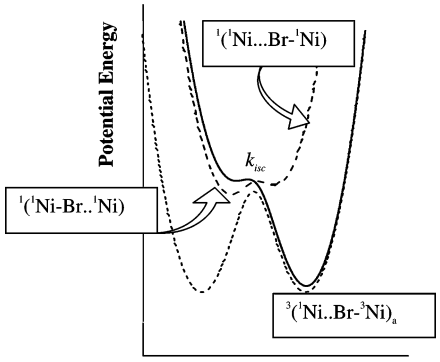

Figure 10. Qualitative model for $[\{L^{(2)}Ni_2\}Br(ClO_4)]^{2+}$. Thermal population of the singlet state (dashed curve) would reduce the overall magnetic moment. The ground-state PE curve for $[L^{(2)}Ni_2Br_3]^+$ is included for comparison (dotted line).

the Ni−X distance for small displacements from the center along this axis. Since there is no net ^{1}Ni−Br covalent bonding contribution, the net interaction between the bridging bromide and ^{1}Ni is repulsive, while there is a net electrostatic attraction for the external bromide. Thus, the external ^{1}Ni−Br bond will be shorter than the bridging ^{1}Ni−Br bond, and this pattern of Ni−Br bond lengths will be reversed for the ^{3}Ni−Br bonds.

These same considerations, combined with the thermally activated configurational interchange account for the transition from the 100 K tetramer structure of $\{[L^{(2)}Ni_2Br_2]^{2+}\}_n$ to the highly symmetrical ambient structure. When the temperature is high enough that there is a significant amount of configurational interchange, there will be a significant probability that one (or both) of the ^{3}Ni^{II} centers of the adjacent dinickel moieties of a tetramer have a low-spin configuration, and the resulting replacement of a weak stabilizing energy by a repulsion will tend to drive the two dinickel moieties apart.

The overall decrease of magnetic moment for increasing temperatures above about 100 K observed for the asymmetric $[L^{(2)}Ni_2(Br)(ClO_4)]^{2+}$ complex is also consistent with the above model since the very weak axial bonding at the Ni′ center will lead to relatively high energies for electronic configurations **3** and **4**, while configuration **2** would be at a lower energy for this complex than for the tribromide ($\epsilon(\sigma_{ClO_4}) \ll \epsilon(\sigma_{Br})$ in eqs 6 and 7); this is illustrated in Figure 10 and supported by the temperature dependence of the magnetic susceptibility data.[69] Thermal population of configuration **2** would then reduce the fraction of paramagnetic species. The observation that a similar temperature-dependent behavior is not observed for $[L^{(2)}Ni_2(Cl)(ClO_4)]^{2+}$ is readily attributable to $\epsilon(\sigma_{Cl}) > \epsilon(\sigma_{Br})$ and the correspondingly higher energy of configuration **2** in this complex.

Conclusions

Our magnetic susceptibility measurements demonstrate that the chloro- and bromo-bridged dinickel complexes contain one high-spin and one low-spin Ni^{II} center per complex at all temperatures. However, there are dramatic changes between the solid-state structures determined at 100 and 300 K for the relatively symmetrical $[L^{(2)}Ni_2Br_3]^+$ and $[L^{(2)}Ni_2Br_2]^{2+}$ complexes: The low-temperature structures have well-defined high- and low-spin Ni^{II} coordination sites within each dinickel moiety, but the Ni^{II} coordination sites are indistinguishable in the ambient structures of both complexes. Moreover, $[L^{(2)}Ni_2Br_2]^{2+}$ is stereochemically strained, and the dinickel moieties are regularly spaced in the ambient structure but associated as tetramers with a larger unit cell volume per complex at 100 K. A thermally activated interchange of the electronic configurations between the Ni^{II} centers of these complexes is implicated by the observations. Since the Ni^{II}−ligand bond lengths are different for the triplet and singlet electronic configurations, the interchange of these electronic configurations between Ni^{II} centers is inseparable from the correlated vibrational motions. The intracomplex configurational interchange can be accomplished by activation of a skeletal vibrational mode, but it may also involve configurational mixing with low-energy electronic excited states. These simple systems are unique examples of vibronically coupled configurational changes in chemical systems, and the facile singlet−triplet configurational interchange between equivalent Ni^{II} centers is an example of triplet excitation transfer in the limit weak electronic coupling and of equal donor and acceptor energies.

In addition, this weak D/A coupling appears to be the reason that such substantial temperature-dependent structural changes are observed, and it indicates that halide-bridged ground-state dσ−pσ−dσ superexchange pathways are not intrinsically significant in these systems. Whether these features are unique to this class of bimetallic complexes or are generally the case for halide-bridged donor−acceptor systems remains to be established. It is possible that the bridging-halide facilitation of electron-transfer processes arises from the coupling of the nuclear motion of the bridging halide with the change of electronic configurations, analogous to the observations reported here.

The electronic matrix element for coupling the reactant and product electronic configurations (as in **1** and **3**) in the dinickel complexes is best represented as a function of the correlated vibrational coordinate. These bimetallic complexes are among the simplest and clearest examples of such vibronic coupling.

Acknowledgment. The authors thank the Office of Basic Energy Sciences of the Department of Energy for partial support of this research. We are grateful to Dr. G. M. Tsoi for assistance with the magnetic measurements.

Supporting Information Available: Structural parameters, magnetic fitting parameters, and CIF files. This material is available free of charge via the Internet at http://pubs.acs.org.

IC050147X